

Universitat Politècnica de Catalunya

FACULTAT DE MATEMÀTIQUES I ESTADÍSTICA

EXTRACTING ENERGY FROM URBAN SURFACES

Models Matemàtics de la Tecnologia

Jordi Plótnikov

Bouke Hoekstra

Pol Tibau

Bernat Coderch

Nicolás Martínez

Pau Inglada

Supervisor: Tim Myers

September 2023

Contents

| | | |
|----------|--|-----------|
| 1 | Abstract | 3 |
| 2 | Introduction and motivations | 4 |
| 3 | Modelling the heat distribution in a one-dimensional rod | 5 |
| 3.1 | Standard heat equation in a finite domain | 5 |
| 3.2 | Standard heat equation in a semi-infinite domain | 8 |
| 3.2.1 | Laplace transform | 8 |
| 3.2.2 | solution of the heat equation | 10 |
| 3.3 | Non-homogeneous convection-diffusion heat equation | 11 |
| 4 | Modelling the effect of solar radiation on a city road | 16 |
| 4.1 | Constant term for solar radiation | 16 |
| 4.2 | Varying solar radiation term, and including the <i>albedo</i> | 18 |
| 4.3 | Further extensions of our model | 21 |
| 5 | The complete model for the temperature of water pipes under city road's | 25 |
| 5.1 | Derivation of our complete model | 25 |
| 5.2 | Steady-state solution for our model | 27 |
| 5.3 | Solving an instance of our model | 29 |
| 6 | Alternate approaches during our research | 38 |
| 6.1 | Solving the non-homogeneous heat equation for a concrete structure . . . | 38 |

| | | |
|----------|---|-----------|
| 6.2 | Solving the non-homogeneous heat equation in a semi-infinite domain . . | 40 |
| 7 | Conclusions | 43 |
| 8 | References | 45 |
| 9 | Appendix | 46 |

1 Abstract

In this report, we are going to model the use of water pipes under city roads to extract energy from the surface, therefore reducing the road temperature. Firstly, we model the temperature of a concrete structure due to the effects of solar radiation, and we then use that to model the heat exchange of the water pipe and the concrete. We used analytical and numerical methods to mainly analyze the impact of these parameters on the heating of our model's water pipe: the depth of the pipe, z , the velocity of the water, u , and the radius of the pipe, R .

2 Introduction and motivations

Climate change and global warming are some of the largest and most discussed problems that exist. Recent studies have found, that air pollution kills more than nine million people per year. Furthermore, it has been shown that the average global temperature has been steadily increasing the last century, which is leading to the disturbance of various ecosystems, with a result that many species that live within these systems are being threatened by extinction due to global warming. Global warming is projected to commit over one-third of the Earth's animal and plant species to extinction by 2050 if current greenhouse gas emissions trajectories continue. The effects of climate change and global warming can be catastrophic and some even believe could be what drives the human race till extinction. In this report we will be modelling a solution to one of the contributors to global warming: the urban heat island effect, which is the phenomenon that urban areas experience higher temperatures compared to their rural surroundings. This phenomenon is due to various factors, for example because of the higher buildings that reflect sunlight and prevent wind flow, or because of dark surfaces (asphalt) that absorb significantly more solar radiation. In this report we will be modelling the use of water pipes under city roads to extract energy from the surfaces, thus reducing the urban heat island effect. We will primarily be using partial differential equations to model the manner in which heat moves through different materials and pipes, and eventually we will obtain the following partial differential equation to model the heat distribution in water pipes under a concrete road, due to solar radiation.

$$\boxed{\rho c(\tilde{T}_t + u\tilde{T}_x) = k\tilde{T}_{xx} - \frac{2}{R}h\tilde{T} + \frac{2}{R}hT^c}$$

Where ρ = density, c = specific heat, k = thermal conductivity, R = radius of the pipe, T_c = temperature of the concrete road

3 Modelling the heat distribution in a one-dimensional rod

In this section we will be modelling a important part of our problem. Remember that we want to study the way that water heats up in a pipe due to solar radiation. A reasonable first approach to our problem would be to study the manner in which heat distributes itself in a one-dimensional rod. Firstly we will be studying the simple heat equation in a finite domain, to get a first understanding of how heat distributes itself through a pipe in the most simple case. After that, we will be extending our domain to a semi-infinite domain to see how this will effect our heat distribution. Lastly, we will be adding diffusion to our heat equation, to obtain a more realistic model of how water heats up in a pipe.

3.1 Standard heat equation in a finite domain

In this subsection, we are going to consider a 1-D approximation model that represents a pipe which is being heated from one end. We will assume that the pipe is fully insulated, and thus there is no transfer of energy throughout the length of the pipe, and heat is only lost and won through the ends of the pipe. This is not a realistic model of what we want to model in the global problem of this report, but it will help us get familiarized with how heat distributes itself in objects, and will introduce a method for solving partial differential equations.

So, that being said, consider the following initial value problem (IVP), *non-dimensionalised* with initial and boundary conditions

$$\left\{ \begin{array}{l} T_t = T_{xx} \\ T(0, t) = 1 \\ T_x(L, t) = 0 \\ T(x, 0) = 0 \end{array} \right. \quad (1)$$

where $T = T(x, t)$ is the function that measures the temperature. This models a one-dimensional pipe of length L , where we assume that one end has a fixed temperature, and

the other is fully insulated. Moreover, we assume that the pipe has an initial temperature of zero. We will solve this system analytically.

Let us first define $Q(x, t) := T(x, t) - 1$ to simplify our boundary conditions (and being able to apply separation of variables). Then, for $t > 0$, $x \in (0, L)$ we have

$$\begin{cases} Q_t = Q_{xx} \\ Q(0, t) = Q_x(L, t) = 0 \\ Q(x, 0) = -1 \end{cases} \quad (2)$$

If we now assume that Q is separable, $Q(x, t) = u(x)v(t)$, from the first condition one ends up with

$$\frac{u''}{u} = \frac{v'}{v} = -\lambda, \quad (3)$$

where $\lambda > 0$. From the second condition

$$u(0) = u'(L) = 0 \quad (4)$$

Combining (3) and (4) while solving the ODE, the IVP solution for $u(x)$ is

$$u(x) = b \sin(\sqrt{\lambda}x), \quad b \in \mathbb{R} \quad (5)$$

where $\lambda_k = \left(\frac{(2k+1)\pi}{2L}\right)^2$, $k \in \mathbb{N}$

For $v = v(t)$ one has $v' = -\lambda v$, so

$$v_k = ce^{-\lambda_k t}, \quad c \in \mathbb{R} \quad (6)$$

Then, considering the linear combination of solutions for Q (which still satisfies our equation) one gets

$$Q(x, t) = \sum_{k=0}^{\infty} A_k e^{-\lambda_k t} \sin(\sqrt{\lambda_k}x), \quad A_k \in \mathbb{R} \quad (7)$$

And finally, imposing the initial condition to find the coefficients A_k , we obtain the following

$$\langle -1, \sin(\sqrt{\lambda_k}x) \rangle = A_k \|\sin(\sqrt{\lambda_k}x)\|^2 \quad (8)$$

And conclude that $A_k = -\frac{4}{\pi(2k+1)}$ (we have basically found the *Fourier Series* solution of our PDE with the method of separation of variables).

And finally, we obtain the solution of our IVP, which is the following function for the temperature in the rod:

$$T(x, t) = 1 - \frac{4}{\pi} \sum_{k=0}^{\infty} \frac{e^{-\lambda_k t} \sin(\sqrt{\lambda_k} x)}{2k+1}, \quad \lambda_k = \left(\frac{(2k+1)\pi}{2L} \right)^2 \quad (9)$$

For simplicity we will select the following length of the rod, $L = 1$, to obtain the following plot of the temperature T , at different time values $t \in [0, 1]$. In this graph we can visualize the evolution of the temperature in the tube, and get an indication of if our calculations are correct.

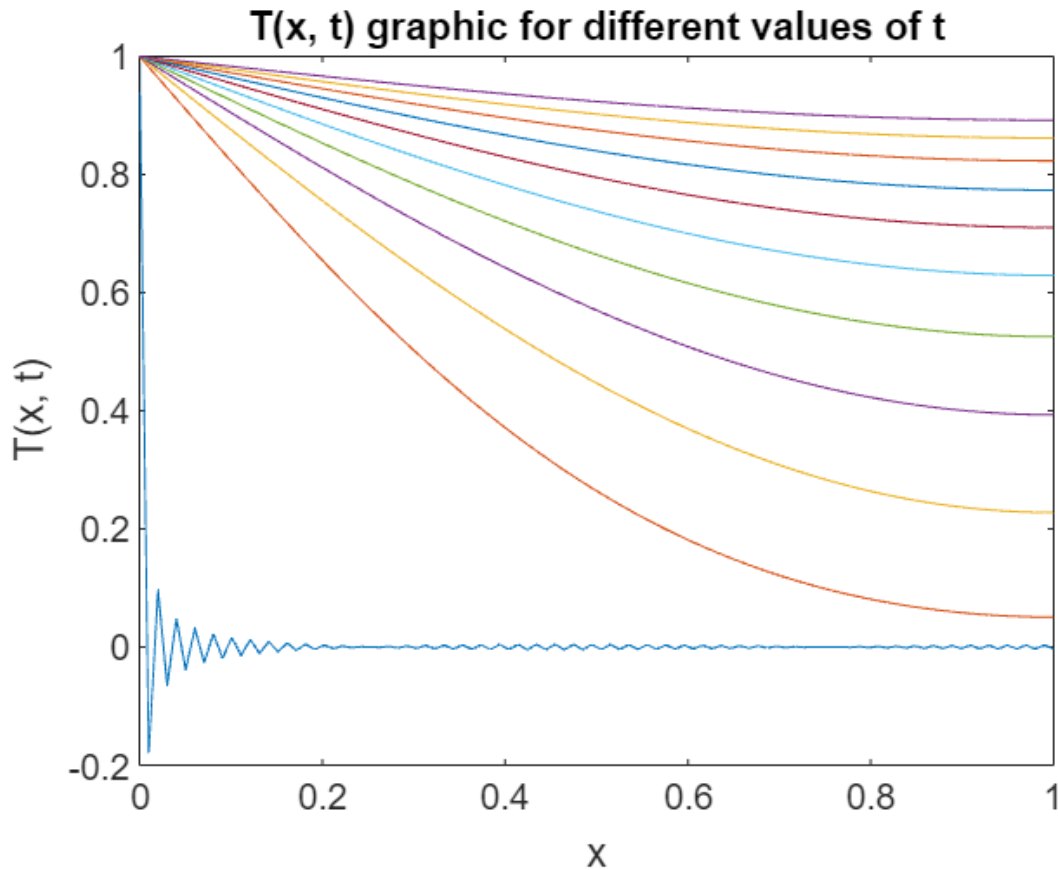


Figure 1: Plot of $T(x, t)$ for $t \in [0, 1]$, $x \in [0, 1]$

We notice that the plot we obtained makes a lot of sense, and this reassures us that the calculations we have made most likely are correct. Notice the following occurrences in

the graph: as time t increases, the temperature T of the tube approaches the value 1, which is the value of the fixed temperature at one end of the rod, and thus we would expect the temperature to finally stabilize at this value. Furthermore, the graph clearly satisfies the boundary conditions of our IVP.

We also notice that for $t \approx 0$, the function starts oscillating and we get an error near 18% in comparison to the limit function. This is due to *Gibbs Phenomenon*, which is a numerical aspect that explains the behaviour of the Fourier series of piecewise continuous functions around jump discontinuities, which is the case that we have at $t \approx 0$.

3.2 Standard heat equation in a semi-infinite domain

In this subsection, we will extend the domain of our heat equation to a semi-infinite domain, and use the so-called *Laplace Transform* to solve this problem.

3.2.1 Laplace transform

As we are now working in a semi-infinite domain, our initial method of solving the heat equation, separation of variables, can no longer be applied. Therefore, we will be introducing a new method to solve partial differential equations (in a semi-infinite domain), which will be the main method of solving PDE's analytically in this report: *the Laplace Transform*. The concept is to transform our function to a different domain, solve it in our often less trouble-some domain, and then use the inverse transform to get the solution in the initial domain. In particular, the Laplace Transform is an integral transform that converts a function of a real variable, into a function of a complex variable. This method is particularly handy, as it allows us to turn our initial partial differential equation, into an ordinary differential equation, which is needless to say less difficult to solve. Moreover, it allows you to solve differential equations with non-bounded domains. The *Laplace transform* is defined as such:

$$\mathcal{L}\{f(t)\} = \int_{t=0}^{\infty} f(t)e^{-st}dt \quad (10)$$

As you can see, the Laplace transform integrates over the variable t , to obtain a function in the variable s . The integral transform possesses a few properties that makes it favourable for solving partial differential equations. Consider the following Laplace transform rules

- $\mathcal{L}\{af(t) + bg(t)\} = a\mathcal{L}\{f(t)\} + b\mathcal{L}\{g(t)\}$
- $\mathcal{L}\{f'(t)\} = sF(s) - f(0)$
- $\mathcal{L}\{\int_0^t f(\tau) d\tau\} = \frac{F(s)}{s}$
- $\mathcal{L}\{e^{at}\} = \frac{1}{s-a}$
- $\mathcal{L}\{f(t) * g(t)\} = \mathcal{L}\{f(t)\} \cdot \mathcal{L}\{g(t)\}$

The rules give us a few useful properties for solving problems. Observe that the transform changes integration into division, and more importantly in our case, it turns differentiation into multiplication. This is favourable because we lose the time derivative in this way. Furthermore, when taking the space derivate for the laplace transform $\mathcal{L}\{\frac{\partial^2}{\partial x^2} f(x, t)\}$, we treat the laplace transform variable t as a parameter, and thus we obtain $\mathcal{L}\{\frac{\partial^2}{\partial x^2} f(x, t)\} = \frac{\partial^2}{\partial x^2} F(x, s)$. Therefore, we can transform partial differential equations with variables t, x into ordinary differential equations with the variables s, x , as we will see in the next subsection. We will demonstrate a simple example, of how you could use the laplace transform to solve a simple differential equation.

Laplace Transform example

Consider the following differential equation with initial condition $y(0) = 0$:

$$\frac{dy}{dt} + 2y = e^{-3t}$$

Step 1: Take the Laplace Transform

$$sY(s) - y(0) + 2Y(s) = \frac{1}{s+3}$$

Step 2: Substitute Initial Condition

$$sY(s) + 2Y(s) = \frac{1}{s+3}$$

Step 3: Solve for $Y(s)$

$$Y(s) = \frac{1}{(s+3)(s+2)}$$

Step 4: Partial Fraction Decomposition

$$Y(s) = \frac{-1}{s+3} + \frac{1}{s+2}$$

Step 5: Inverse Laplace Transform

$$y(t) = -e^{-3t} + e^{-2t}$$

We have now solved our differential equation fairly quickly, using the rules we defined above. In the next part, we will see how we can use the Laplace transform to solve our heat equation extended to an unbounded domain $x \in (0, +\infty)$.

3.2.2 solution of the heat equation

Now that we have introduced the Laplace transform, as a method to solve partial differential equations on non-bounded domains, we will use it to solve the following extension of our initial heat equation to a semi-infinite domain.

$$\begin{cases} T_t = T_{xx} \\ T(0, t) = 1 \\ \lim_{x \rightarrow +\infty} T_x(x, t) = T(x, 0) = 0 \end{cases} \quad (11)$$

The physical interpretation of this model, could be that of a semi-infinite, fully insulated pipe with fixed temperature at the starting end of the pipe. The new boundary condition

we introduce models the assumption that there is no heat exchange far along the pipe. We will apply the *Laplace transform* in the time variable t .

$$\mathcal{L}\{T_t = T_{xx}\} \iff sT(x, s) - T(x, 0) = \frac{\partial^2}{\partial x^2} T(x, s) \quad (12)$$

Using our initial condition, $T(x, 0) = 0$, we derive the following ODE with corresponding boundary and initial conditions:

$$\begin{cases} \frac{\partial^2}{\partial x^2} T(x, s) = sT(x, s) \\ T(0, s) = \frac{1}{s} \\ \lim_{x \rightarrow \infty} T_x(x, t) = 0 \end{cases} \quad (13)$$

Solving the ODE without using the initial condition we get:

$$T(x, s) = Ae^{-x\sqrt{s}} + Be^{x\sqrt{s}} \quad (14)$$

We observe that for $x \rightarrow \infty$, the second term will diverge, and therefore we set $B = 0$. Finally, we impose the initial conditions to obtain the laplace transform solution of our ODE problem:

$$T(x, s) = \frac{e^{-x\sqrt{s}}}{s} \quad (15)$$

Then we merely have to find the inverse Laplace transform of this, to get the solution to our initial PDE problem.

$$T(x, t) = 1 - \operatorname{erf}\left(\frac{x}{2\sqrt{t}}\right) \quad (16)$$

In the graphic below, we have once more plotted the temperature in the rod, for different time values $t \in [0, 1]$, and we observe that it clearly satisfies the boundary conditions, in particular the neumann null condition on the semi-infinite domain. We also notice that even though we have a semi-infinite rod, as the initial temperature is zero, the rod has a temperature of zero from a certain point on:

3.3 Non-homogeneous convection-diffusion heat equation

Now that we have had familiarized ourselves with a simple heat equation to get a better first impression of our problem, we are going to consider a more realistic approach to

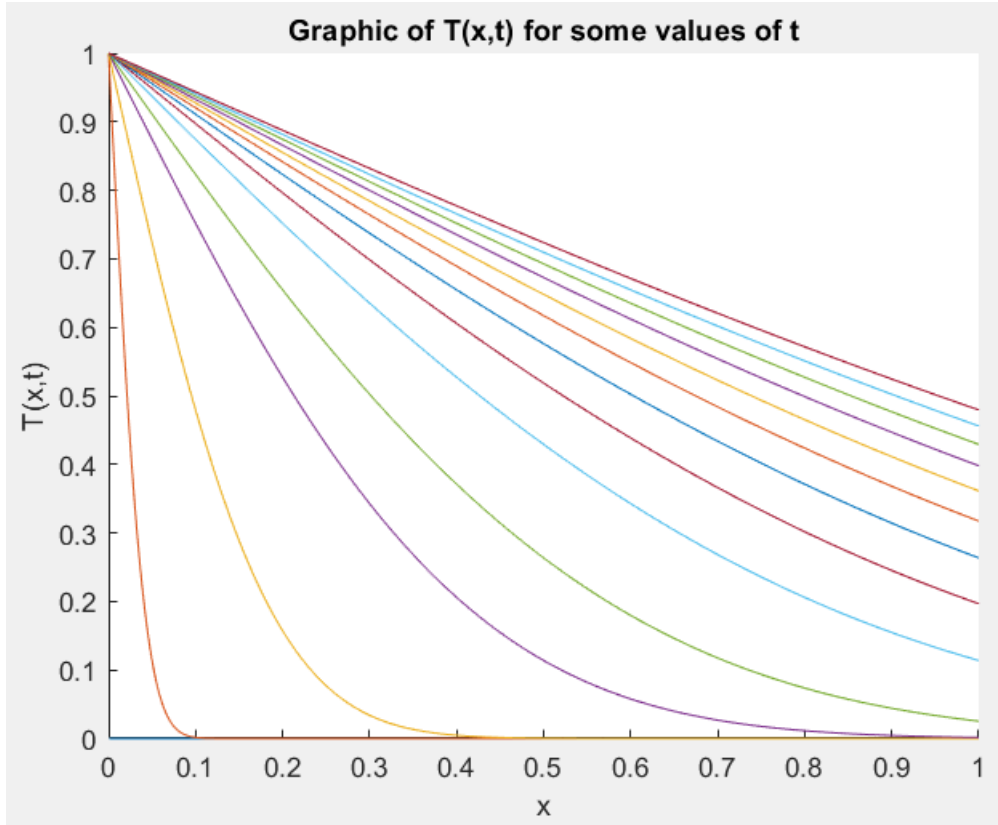


Figure 2: Plot of $T(x, t)$ for $t \in [0, 1]$, $x \in [0, 1]$

model the heat exchange of water in a pipe. We will add a variable to model the convection of the water through the pipe, to obtain a better approximation of the problem that we are trying to model. We will also introduce some parameters based on the physical properties of the materials and the environment considered, and we will introduce a way of “getting rid” of them to simplify our equation.

Consider the following IVP that describes the temperature of a fluid in movement:

$$\begin{cases} \rho c (T_t + u T_x) = k T_{xx} + \frac{2Q}{R} \\ T(0, t) = T_0 \\ T_x(L, t) = 0 \\ T(x, 0) = T_0 \end{cases} \quad (17)$$

where ρ = density of the fluid, c = specific heat, u = velocity of the fluid, k = thermal conductivity, T_0 = initial temperature, L = length of the pipe, Q = heat rate of a source inside the rod, R = radius of the pipe.

This model, models the temperature of a fluid in movement, in a pipe that is fully insulated except in one end, where it has a fixed temperature. Notice that as we have a constant for the length of our pipe, we are working in a finite domain. To simplify this problem, we are going to *non-dimensionalize* our equation to obtain another equation with fewer parameters. Firstly, let us define

$$\hat{T} := \frac{T - T_0}{A}, \quad \hat{t} := \frac{t}{B}, \quad \hat{x} := \frac{x}{C} \quad (18)$$

where A, B, C are temperature, time and position scales, respectively. Our equation can now be written as

$$\frac{A}{B} \hat{T}_{\hat{t}} + \frac{uA}{C} \hat{T}_{\hat{x}} = \frac{kA}{\rho c C^2} \hat{T}_{\hat{x}\hat{x}} + \frac{2Q}{\rho c R} \quad (19)$$

After rearranging the parameters, one can achieve the following

$$\frac{C}{uB} \hat{T}_{\hat{t}} + \hat{T}_{\hat{x}} = \frac{k}{u\rho c C} \hat{T}_{\hat{x}\hat{x}} + \frac{2QC}{\rho c u R A} \quad (20)$$

Taking now $C = \frac{k}{u\rho c}$, $B = \frac{k}{u^2\rho c}$, $A = \frac{2kQ}{u^2\rho c R}$, as our scales, we can reduce our problem to the following simpler IVP, where the parameters are contained in our variables.

$$\begin{cases} \hat{T}_{\hat{t}} + \hat{T}_{\hat{x}} = \hat{T}_{\hat{x}\hat{x}} + 1 \\ \hat{T}(0, \hat{t}) = 0 \\ \hat{T}_{\hat{x}}(\hat{L}, \hat{t}) = 0 \\ \hat{T}(\hat{x}, 0) = 0 \end{cases} \quad (21)$$

In our IVP $\hat{L} = \frac{L}{C}$, but for now we will set this constant to $\hat{L} = 1$ for simplicity. The parameters could take the following realistic real-world values, $k = 1.46 \cdot 10^{-7} m^2/s$, $R \in [5, 20] cm$, $T_0 = 293K$, $u \in [1, 10] cm/s$, $Q = 400W/m^2$. For simplicity, We will use the abuse of notation $\hat{x} = x$, $\hat{t} = t$. As we wanted, we have eliminated all the laborious constants and have left only the *essence* of the equation.

We will firstly solve the IVP numerically and plot the graph of our scaled temperature \hat{T} , and then we will see an analytical approach to solve the problem. Using the *Matlab* code shown in the appendix, which uses the *pdepe* package (made for solving numerically 1-D

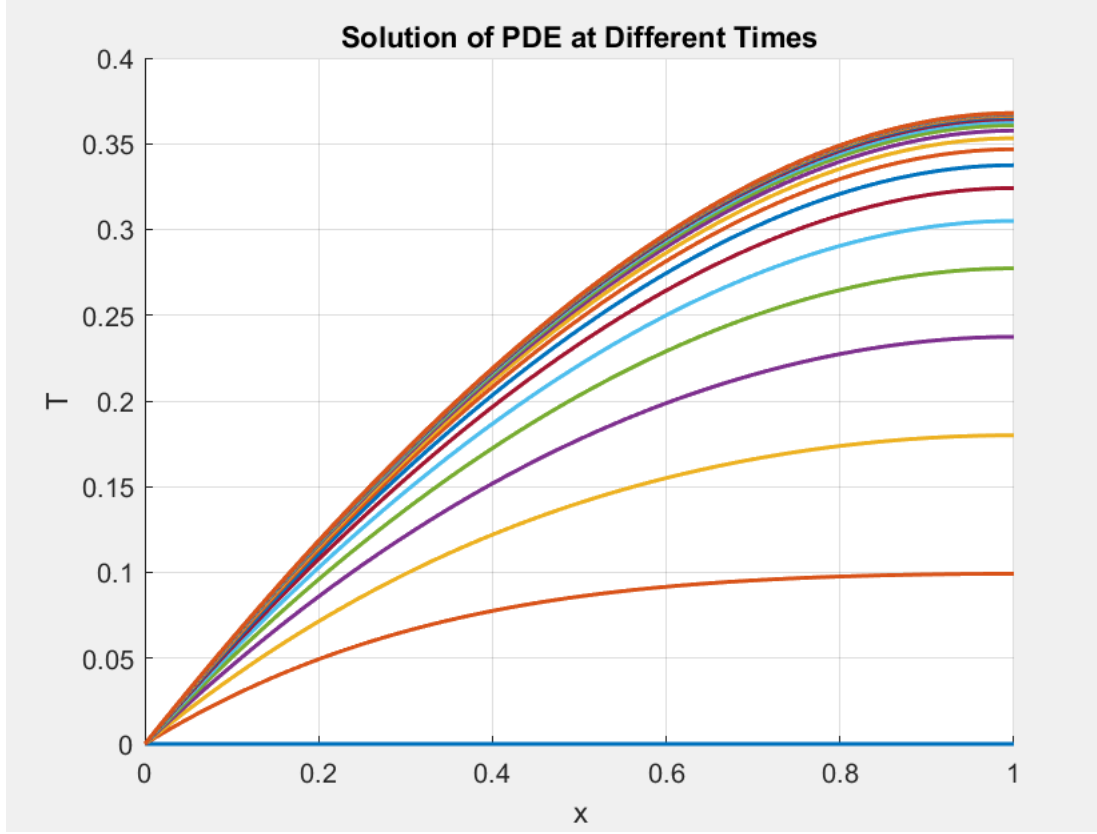


Figure 3: Plot of $\hat{T}(\hat{x}, \hat{t})$ for $\hat{t} \in [0, 10]$, $\hat{x} \in [0, 1]$

parabolic and elliptic PDE's) we obtained the following graph for the scaled temperature at different times $\hat{t} \in [0, 10]$:

Analyzing the graph, we observe that it clearly verifies the boundary conditions, and more importantly, we notice that, as time tends to infinity, $\lim_{t \rightarrow +\infty} \hat{T}(1, t) \approx 0.37$, so the temperature at the end of the rod stabilizes to a certain value after some time. We will explain this analytically.

Consider the following simplification of our non-dimensionalized equation,

$$\begin{cases} \hat{T}_x = \hat{T}_{xx} + 1 \\ \hat{T}(0, t) = 0 \\ \hat{T}_x(1, t) = 0 \end{cases} \quad (22)$$

which corresponds to the steady state, $\hat{T}_t \rightarrow 0$ as $t \rightarrow +\infty$. Hence, the two solutions must coincide for $t \gg 0$, as for large times, our system stabilizes. This time-independent IVP

is easily solved analytically.

We interpret and solve our IVP as an ODE, proceeding by an easy separation of variables, and imposing the boundary conditions.

$$\hat{T}(x, t) = \hat{T}(x) = x - e^{x-1} + \frac{1}{e} \quad (23)$$

Note that, in this case, as our equation is time-independent, \hat{T} depends only on x . It is easy to see that $\lim_{t \rightarrow +\infty} \hat{T}(1, t) = 1/e \approx 0.37$, which agrees with what we saw numerically. Consider the graph below, that we use to compare our numerical and analytical solutions.

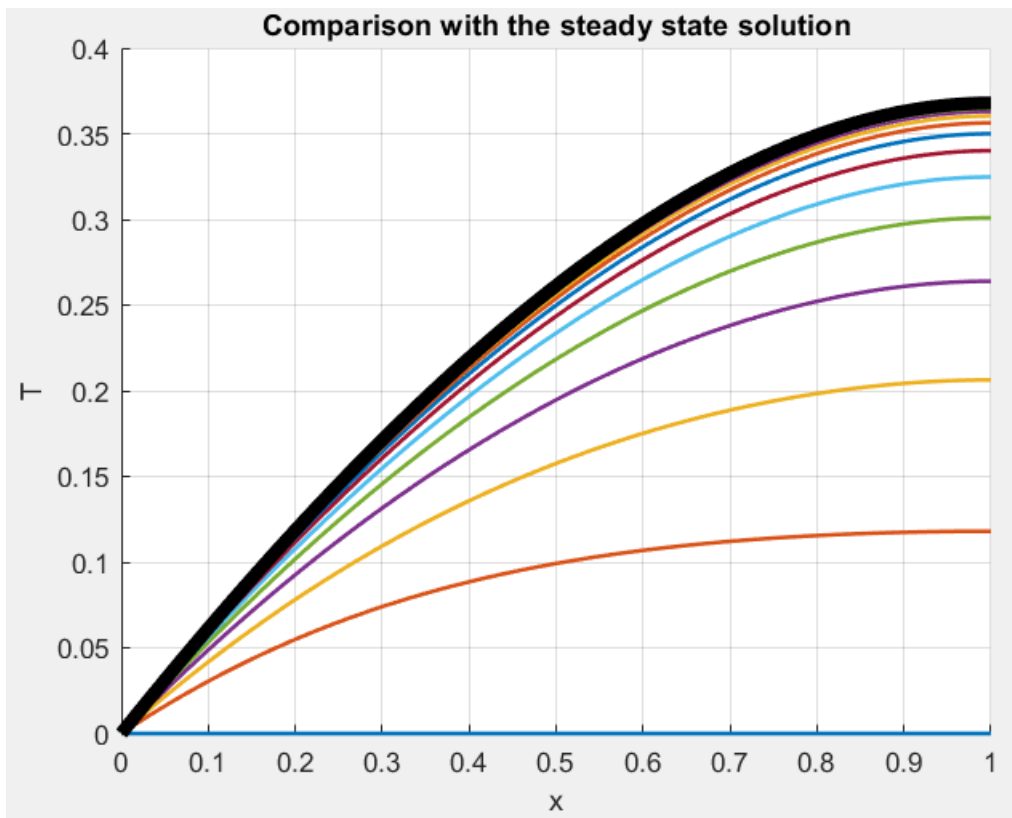


Figure 4: Comparison of the two plots

The coloured lines represent the numerical solution of the PDE for different times $t \in [0, 10]$, and the thick black line corresponds to the analytical solution of the ODE. Notice that as time tends to infinity, $\lim_{t \rightarrow +\infty} \hat{T}(x, t)$ our numerical solution approaches our analytical solution.

4 Modelling the effect of solar radiation on a city road

Remember the global problem that we are attempting to model: we want to model a solution to the urban heat effect, using water pipes under city road's to extract energy and heat from the surface. In order to do this we need to model the heat distribution in water pipes under city road's, where in this report we assume that the surface absorbs all it's energy from solar radiation. We have now modelled the heat distribution of fluid in motion in a pipe, but we still need to incorporate the effect of solar radiation to heat up our pipe. We will start by modelling the heat distribution of a solid structure (road), with constant solar radiation, and afterwards we will incorporate a more realistic solar radiation term that varies throughout the day. .

4.1 Constant term for solar radiation

We will now construct our attempt to model the effect of solar radiation on a road. As we want to get a first understanding of the problem, we will simplify our problem and assume in this model that the solar radiation is constant throughout the day. Therefore this model is not a good approximation of the solar effect throughout a whole day, but it could be a reasonable approximation of the effect of solar radiation in a smaller period of time. Consider the following IVP describing temperature variation in a solid structure

$$\begin{cases} \rho c T_t = k T_{zz} \\ -k T_z(0, t) = Q_{sun} \\ \lim_{z \rightarrow +\infty} T_z(z, t) = 0 \\ T(z, 0) = T_\infty \end{cases} \quad (24)$$

Where ρ = density, c = specific heat, k = thermal conductivity, Q_{sun} = solar heat rate, T_∞ = initial heat distribution

In this IVP, $T(z, t)$ models the temperature of the road at depth z and time t , we assume

that the heat exchange at the surface is constant, and that there is no heat exchange deep in our surface.

Notice that we are operating on a semi-infinite domain once again, and thus we will be working with the *Laplace transform* method explained before once more. We use this method to obtain the following Laplace equivalent to our problem.

$$\begin{cases} \rho c(s\hat{T}(z, s) - T_\infty) = K\hat{T}_{zz}(z, s) \\ -K\hat{T}_z(0, s) = \frac{Q_{sun}}{s} \\ \lim_{z \rightarrow +\infty} \hat{T}_z(z, s) = 0 \end{cases} \quad (25)$$

Solving this, we achieve the following Laplace solution

$$\hat{T}(z, s) = \frac{Q_{sun}}{s\sqrt{s}\sqrt{\rho c K}} e^{-\sqrt{s\frac{\rho c}{K}}z} + \frac{T_\infty}{s} \quad (26)$$

And, finally, applying the inverse Laplace transform to get the solution to the initial problem, we obtain the following solution to our IVP:

$$\boxed{\mathcal{L}_s^{-1}(\hat{T}(z, s))(t) = T(z, t) = \frac{2\sqrt{t}Q_{sun}e^{-\frac{\rho c z^2}{4Kt}}}{\sqrt{\rho c K}\sqrt{\pi}} - \frac{zQ_{sun}}{K}\text{erfc}\left(\frac{z\sqrt{\rho c}}{2\sqrt{tK}}\right) + T_\infty} \quad (27)$$

Where $\text{erfc}(x) = 1 - \text{erf}(x)$. In the graph below, we plot the temperature throughout the structure, at different times t (interval of approximately 4 hours), using usual real-world values of concrete for the parameters. Note that the temperature, T , is expressed in *kelvin*. The graph obtained agrees with our initial value problem in the following way:

As time increases, the concrete structure keeps heating up further, but as we get deeper in our surface the temperature persistently decreases to 0. This is the expected behaviour according to our model, and if we varied the parameters we would be able to see how each constant affects the modelling. The model we constructed, however, does not take into account the variance of radiation from the sun along the day, or how the darkness of a surface affects the heating of the structure, for example.

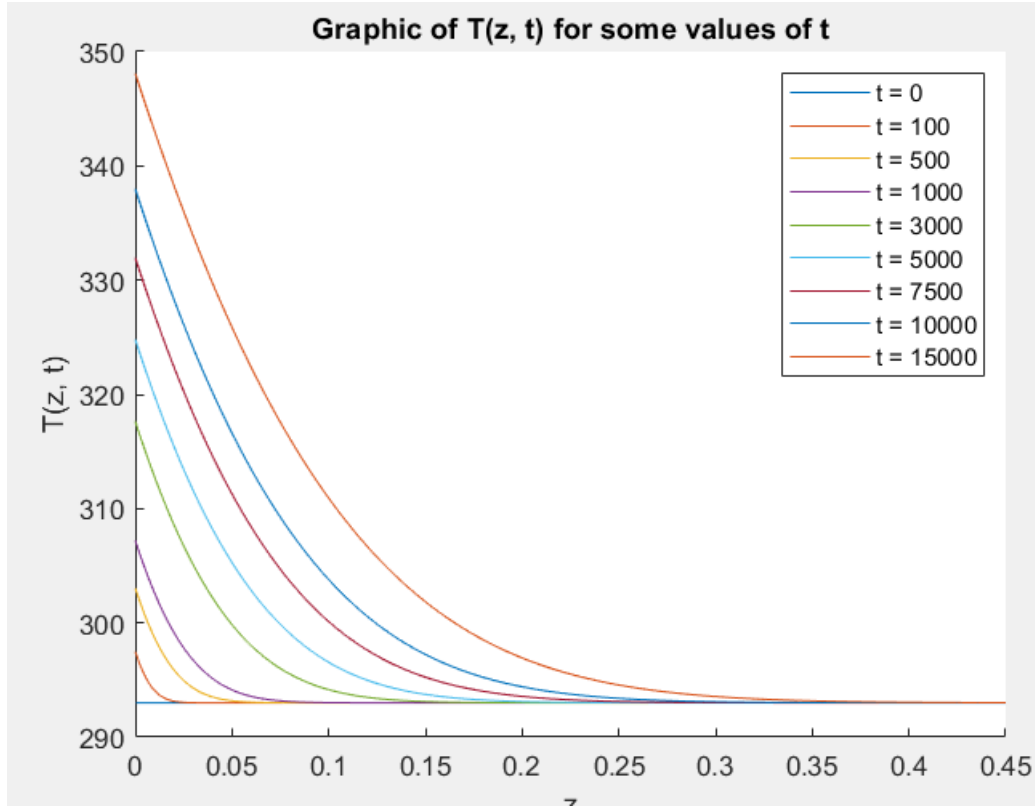


Figure 5: Plot of $\hat{T}(z, t)$ (in *kelvin*) for $t \in [0, 10000]s$, $z \in [0, 0.45]$

4.2 Varying solar radiation term, and including the *albedo*

To incorporate the occurrence that solar radiation varies throughout the day, we let our solar radiation term be time-dependent, $Q_{sun} = Q_{sun}(t)$. A first approach to model this term, could be to consider the following function for the heat rate rate of the sun, $Q_{sun}(t) = Q_{max} \sin\left(\frac{2\pi t}{p}\right)$, where p describes the period of the sun. We will model the solar radiation on a clear sunny day in the summer. We assume that the sun rises at 6 a.m. and sets at 10 p.m, moreover we assume that the solar radiation is the strongest at 2 p.m. to obtain the following function: $Q_{sun}(t) = 800 \sin\left(\frac{2\pi(t-6)}{32}\right)$, with maximum heat rate value $Q_{max} = 800$ (at 2 p.m)

This is a far more realistic approximation, but it gives rise to some difficulties while calculating its Laplace- and inverse Laplace transform. We solved this problem by approximating our sinus function by a quadratic function. We approximated the sinus function by the parabola seen in the graph below, where the parabola also has zeros at $t_0 = 6h$ and $t_f = 22h$, and maximum value 800 at $t_{mid} = 14h$.

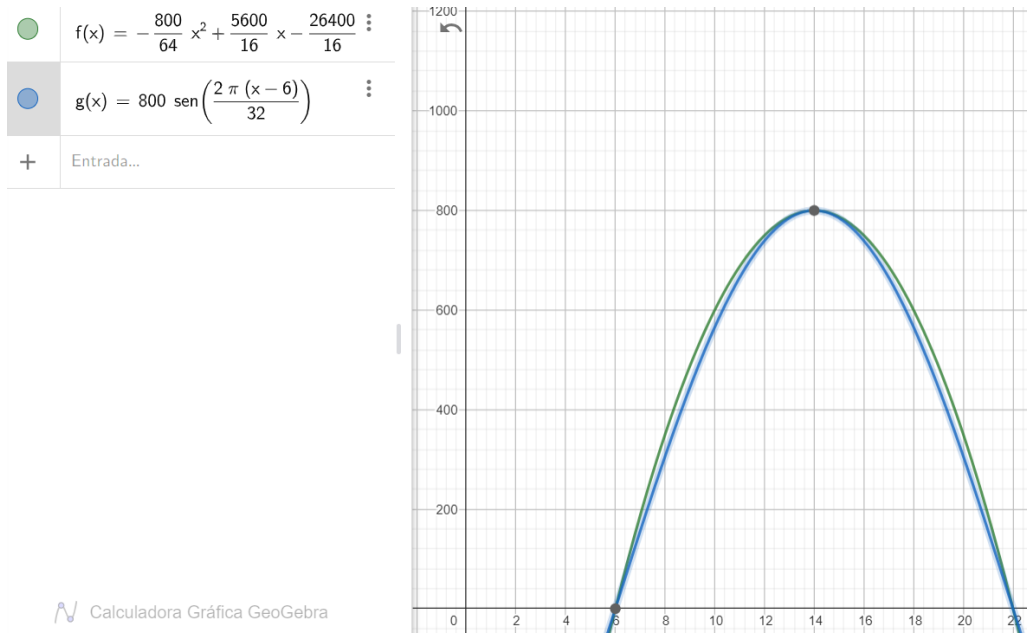


Figure 6: Comparison between the two considered approximations for $Q_{sun}(t)$

As you can see, the parabola is a reasonable approximation to our sinus function, and computing the Laplace transformation of our quadratic function should not be a problem, therefore we use the following quadratic function for the heat rate: $Q_{sun}(t) = -\frac{25}{2}t^2 + 350t - 1650$

Another occurrence that we want to incorporate into our model, is the effect that darker surfaces absorb much more heat than lighter surfaces. To do this, we are going to include the *albedo* term in our model, the albedo gives the fraction of light reflected from a surface. Therefore, darker surfaces have low albedo, and don't reflect a lot of light, and therefore heat up faster. Lighter surfaces have higher albedo, they reflect a larger proportion of the light, thus resulting in a cooler surface temperature. In the table below we see the *albedo* values $a_s \in [0, 1]$ for different surface materials, s , commonly used in city road's

| Material, s | <i>Albedo</i> value, a_s |
|---------------|----------------------------|
| Concrete | 0.20 - 0.45 |
| Asphalt | 0.05 - 0.20 |
| Brick, stone | 0.20 - 0.40 |
| White paint | 0.50 - 0.90 |
| Black paint | 0.05 |

Obviously $(1 - a_s)$ gives us the fraction of light that a surface absorbs, and thus we will be incorporating this term in our model.

With these two modifications we have further extended our model, to obtain a more realistic approximation of the effect of solar radiation on a solid structure. In the graph's below we plot the temperature throughout the structure for asphalt, and for concrete structures. We used a translation on the polynomial, to start at $t_0 = 0s$ and finish at $t_f = 16 \cdot 3600s$, instead of $t_0 = 6 \cdot 3600s$, $t_f = 22 \cdot 3600s$, and introduced $W = Q_{sun}(t_0) = Q_{sun}(t_f)$, as Q_{sun} at night is small but not zero, in the figure below we assumed $W = 5$.

The full (and large) expressions corresponding to the analytical solutions to the problem, $\hat{T}(z, t)$, can be found in the appendix. Due to its complexity we decided not to include it here.

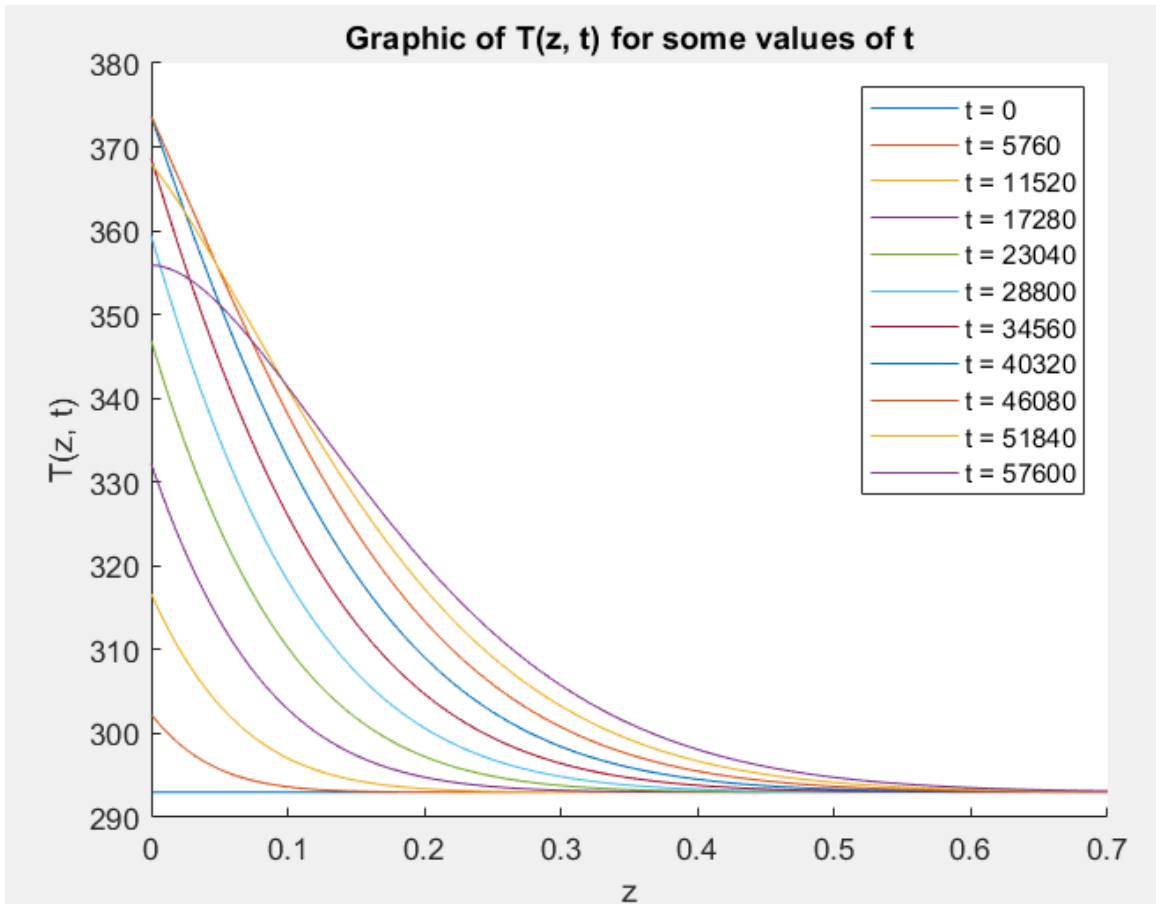


Figure 7: Graphic for asphalt, *albedo* value, $a_s = 0.05$ (complete interval of 16h)

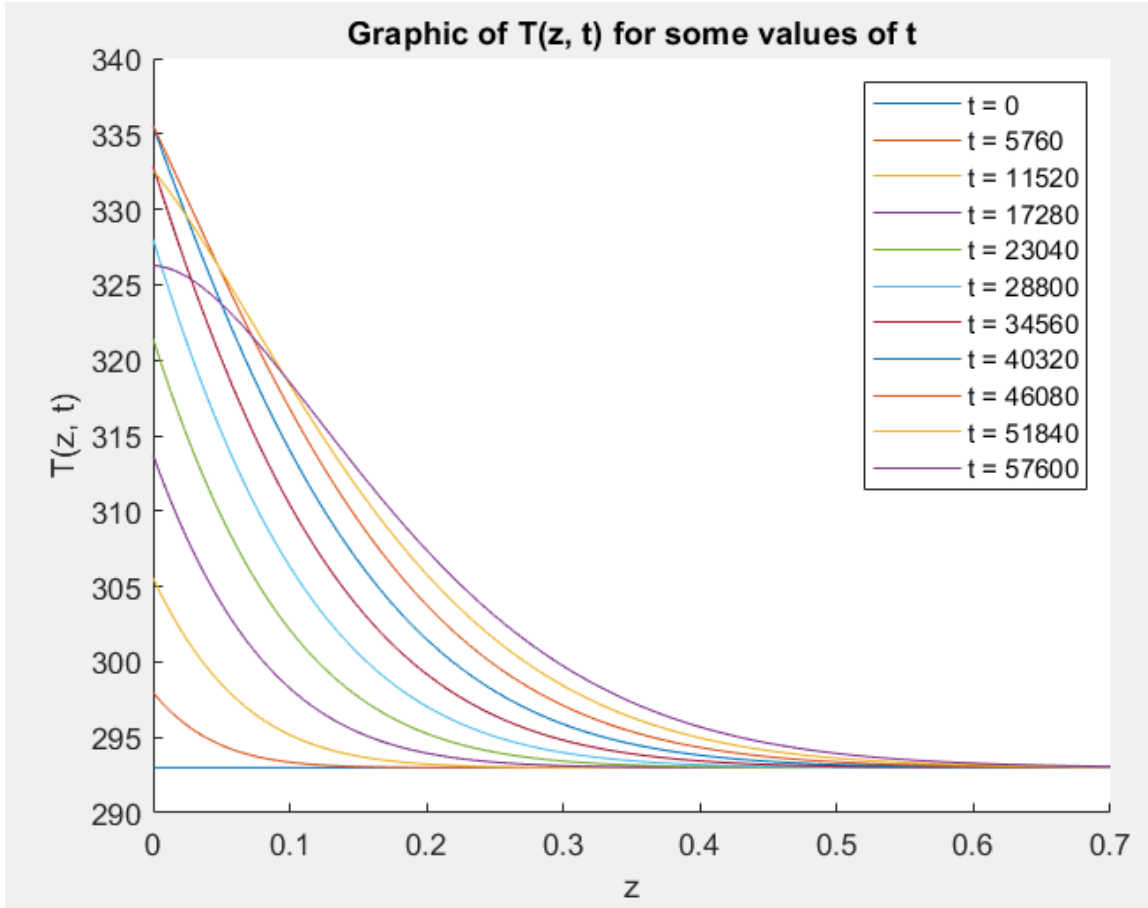


Figure 8: Graphic for concrete, *albedo* value, $a_s = 0.5$ (complete interval of 16h)

Clearly, the functions satisfy the boundary conditions and as expected, for the higher *albedo* value of the concrete, the temperature reached is smaller, and the darker surfaces asphalt absorbs more energy from the sun.

4.3 Further extensions of our model

In the solar radiation term in the last subsection, we were restricted to the modelling of the sunlight hours of a single day (6 a.m. - 10 p.m). We can further extend the solar radiation term, to consider longer periods of time, which could give us a better understanding of how the city road's cool off during the night for example. This extension can be accomplished by considering a (periodic) *Fourier series* as in the following function

$$Q_{sun}(t) = \begin{cases} W & , \quad \text{if } 0 \leq t \leq 4 \\ \frac{W-Q_M}{64}t^2 + \frac{3(Q_M-W)}{8}t + \frac{9W-5Q_M}{4} & , \quad \text{if } 4 < t < 20 \\ W & , \quad \text{if } 20 \leq t \leq 24 \end{cases} \quad (28)$$

where $Q_M = Q_{max}$. One should fix the time units in order to apply this term in the model correctly, but to visualize it, with usual values for W and Q_M , the solar radiation function behaves as follows

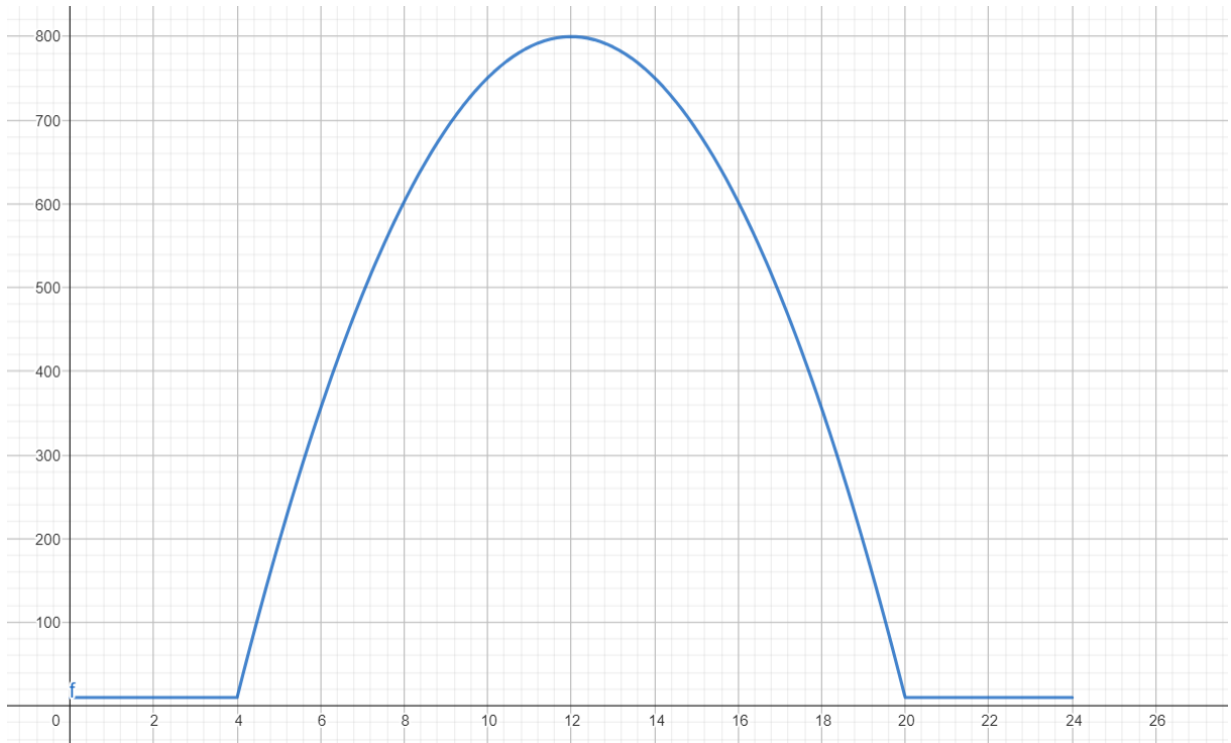
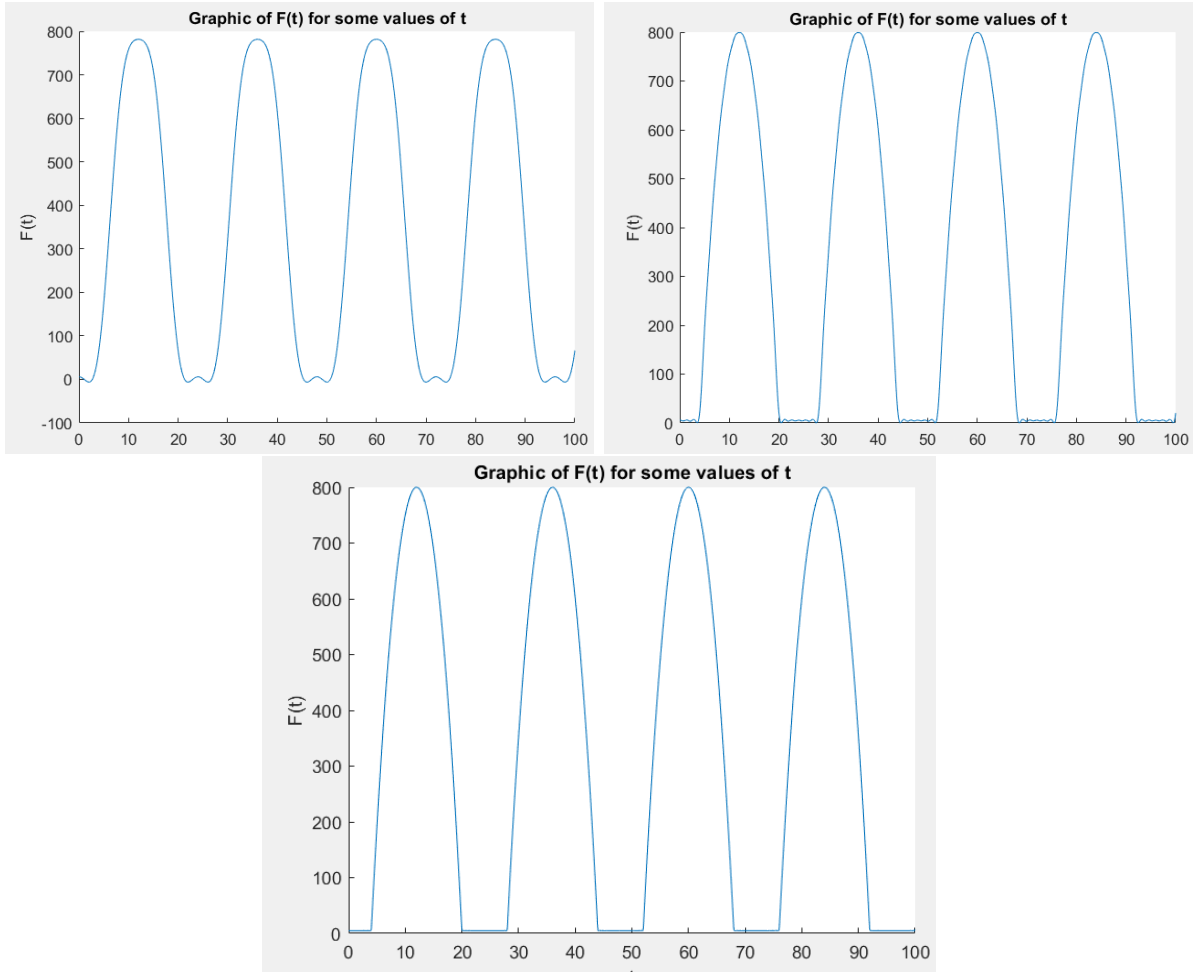


Figure 9: Graphic representation of the function to consider the periodic extension of
(here $Q_M = 800W/m^2$, $W = 10W/m^2$)

If we compute the *Fourier series* of the previous function and plot it for different series values n , the results are as follows



Figures 10-12: Periodic *Fourier Series* of the function modelling $Q_{sun}(t)$ for $n = 3, n = 15, n = 150$ (here $Q_M = 800W/m^2, W = 5W/m^2$)

As expected, the *Fourier Series* of $Q_{sun}(t)$ gives us a very accurate approximation for large n of the periodic extension of the function, which can be considered as a Q_{sun} modelling multiple days. Even though the application of this last extension of our radiation term on our complete model would be very interesting, as it would allow us to analyze the behaviour of the model for longer periods of time, we will not apply it due to restrictions on time and complexity of our model (basically, difficulty of computing the *inverse Laplace transform*), therefore we will stick to the polynomial solar radiation term in the remainders of this report.

In our IVP from the start of this chapter, we have assumed for simplicity that the initial temperature of the road is not dependent on the depth. This is not very realistic of course, as the temperature close to the surface is always higher than at higher depths.

Another realistic extensions of our IVP, could be to take this effect into account in the initial condition $T_\infty = T_\infty(z)$. Unfortunately, we lack the time and resources to implicate this extension, as we would need a new method to solve this IVP, as this extension complicates the computation of the *Laplace transforms*.

5 The complete model for the temperature of water pipes under city road's

We have now successfully modelled the heat exchange of water in a pipe, and modelled the effect of solar radiation on city road's. In this section, we are going to combine these models to obtain the main model of this report. Remember that we are modelling the effect of water pipes under city roads to extract energy from the surfaces, thus reducing the urban heat island effect. Therefore, we are going to model the heat distribution in water pipes under a concrete road, due to solar radiation. We have chosen the material concrete for our road, as it has a more favourable albedo value than asphalt. In this model, we will assume the pipe to be cylindrical and located in a solid concrete road structure at the depth H .

5.1 Derivation of our complete model

In this subsection, we will derive the complete model for our problem. We will make a few assumptions, namely that there are no sources or sinks, our fluid is incompressible, and that the diffusion coefficient is constant. We will also assume that the temperature in the pipe is radially symmetric in the radius, r , thus obtaining the temperature function $T = T(r, x, t)$. As we are not working in one-dimension anymore, we obtain the following adjustment of our previous model of heat distribution of a fluid in movement in a pipe,

$$\rho c(T_t + \mathbf{u} \cdot \nabla T) = k \Delta T \quad (29)$$

Since the fluid we are studying is water, we have that its density is $\rho = 998 \text{ kg/m}^3$ and its dynamic viscosity is $\mu = 8.90 \cdot 10^{-4} \text{ Pa} \cdot \text{s}$. In a regime of velocities $u \in (0.01 \text{ m/s}, 0.1 \text{ m/s})$ and with a characteristic length $L > 1$, we will have a high Reynolds number $Re = \frac{\rho u L}{\mu} > 10^6$ leading to turbulent flow. Therefore, the fluid is going to be well mixed and thus we can consider an average constant velocity $\mathbf{u} = (u, 0, 0)$. Using the expression for the Laplacian in cylindrical coordinates we get the convection-diffusion equation for a fluid's

temperature:

$$\rho c(T_t + uT_x) = k \left(\frac{1}{r} \frac{\partial}{\partial r} (rT_r) + T_{xx} \right) \quad (30)$$

Averaging now over the cross-section, we obtain:

$$\rho c \int_0^{2\pi} \int_0^R (T_t + uT_x) r dr d\theta = k \int_0^{2\pi} \int_0^R \left(\frac{1}{r} \frac{\partial}{\partial r} (rT_r) + T_{xx} \right) r dr d\theta \quad (31)$$

and define the average temperature over the cross-section

$$\tilde{T} := \frac{1}{\pi R^2} \int_0^{2\pi} \int_0^R T_r dr d\theta \quad (32)$$

to obtain

$$\rho c(\tilde{T}_t + u\tilde{T}_x) = k\tilde{T}_{xx} + k\frac{2}{R} T_r|_R \quad (33)$$

At the outer boundary of the pipe $r = R$, the boundary condition states

$$-k T_r|_R = h(T|_R - T^c) \quad (34)$$

where $T^c = T^c(H, t)$ is the temperature of the concrete structure (road) at the height H . This states that the heat exchange at the outer boundary of the pipe, is proportional to the difference in temperature of the pipe and the surrounding concrete.

If the fluid is well-mixed we can assume that $T|_R = \tilde{T}$. Using that, we finally obtain the following convection-diffusion equation to model the temperature distribution of flowing water in pipes under a concrete road

$$\boxed{\rho c(\tilde{T}_t + u\tilde{T}_x) = k\tilde{T}_{xx} - \frac{2}{R}h\tilde{T} + \frac{2}{R}hT^c} \quad (35)$$

In order to completely define our model, we need to add two boundary conditions and one initial condition. Therefore, our complete model will be

$$\begin{cases} \rho c(\tilde{T}_t + u\tilde{T}_x) = k\tilde{T}_{xx} - \frac{2}{R}h\tilde{T} + \frac{2}{R}hT^c \\ \tilde{T}(0, t) = T_0 \\ \tilde{T}(x, 0) = T_0 \\ \lim_{x \rightarrow \infty} \tilde{T}_x = 0 \end{cases} \quad (36)$$

5.2 Steady-state solution for our model

In this section, we delve into the steady-state analysis of the convection-diffusion equation applied to a water pipe scenario. The focus is on understanding the temperature distribution within the pipe under steady-state conditions. The governing equation, that we have just derived, is presented as:

$$T_t + uT_x = DT_{xx} - A(T - T^c) \quad (37)$$

where T is water's temperature, $D = \frac{k}{\rho c}$ is the diffusion coefficient, $A = \frac{2h}{R\rho c}$ is a physical constant and $T^c = T^c(H, t)$ is concrete's temperature at depth H .

Since we are considering a steady-state solution, we have that $T_t = 0$, so we reduce the equation to a second-order ordinary differential equation (ODE). The boundary conditions are defined as $T(0, t) = T_{ini}$ and $\lim_{x \rightarrow \infty} T_x = 0$. To facilitate the analytical approach, we will once more non-dimensionalize our equation to simplify it.

Let us define the non-dimensional scaled variables

$$\hat{T} = \frac{T - T_{ini}}{\Delta T} \quad \text{and} \quad \hat{x} = \frac{x}{L}, \quad \text{where} \quad L = \frac{u}{A} \quad \text{and} \quad \Delta T = T^c - T_0 \quad (38)$$

Using these new variables, we transform our equation into the following

$$\begin{cases} \frac{DA}{u^2} \hat{T}_{\hat{x}\hat{x}} - \hat{T}_{\hat{x}} = \hat{T} - 1 \\ \hat{T}(0, t) = 0 \\ \lim_{\hat{x} \rightarrow \infty} \hat{T}_{\hat{x}} = 0 \end{cases} \quad (39)$$

Furthermore, let us assume that $\frac{DA}{u^2}$ is a small number, so that we can write

$$\varepsilon = \frac{DA}{u^2} \quad \text{where} \quad 0 < \varepsilon \ll 1. \quad (40)$$

Therefore, the solution changes rapidly in a very small layer, say of width $\mathcal{O}(\varepsilon)$, but is smooth elsewhere. Such a small layer is known as a boundary layer. The idea is to find an outer expansion of the solution valid away from the boundary layer, $\hat{x} \gg \mathcal{O}(\varepsilon)$, and an inner expansion valid in the boundary layer. Finally, matching both expansions we will have a good description of the full solution without actually having to find it.

Outer expansion Expanding the solutions in powers of ε

$$\hat{T} = \hat{T}_0 + \hat{T}_1\varepsilon + \dots$$

we have that

$$\varepsilon \left(\hat{T}_{0_{\hat{x}\hat{x}}} + \hat{T}_{1_{\hat{x}\hat{x}}}\varepsilon + \dots \right) - \left(\hat{T}_0 + \hat{T}_1\varepsilon + \dots \right) + 1 = \hat{T}_{0_{\hat{x}}} + \hat{T}_{1_{\hat{x}}}\varepsilon + \dots$$

Since $\varepsilon \ll 1$, the leading order outer problem is

$$\hat{T}_{0_{\hat{x}}} = -\hat{T}_0 + 1$$

and thus the outer expansion is

$$\hat{T}(\hat{x}) = \hat{T}_0(\hat{x}) = c_0 e^{-\hat{x}} + 1, \quad c_0 \in \mathbb{R}$$

only valid if $\hat{x} \gg \mathcal{O}(\varepsilon)$. Note that this expansion clearly satisfies the outer boundary condition $\lim_{\hat{x} \rightarrow +\infty} \hat{T}_{\hat{x}} = 0$.

Inner expansion We can investigate the behaviour near the origin more closely by rescaling \hat{x} and \hat{T} in the boundary layer, writing $\hat{x} = \varepsilon^\alpha \bar{x}$ and $\hat{T} = \varepsilon S$. Then, the rescaled problem is

$$\begin{cases} \varepsilon^{2-2\alpha} S_{\bar{x}\bar{x}} - \varepsilon S + 1 = \varepsilon^{1-\alpha} S_{\bar{x}} \\ S(0) = 0 \end{cases}$$

Choosing $\alpha = 1$ to balance the terms and letting $\varepsilon \rightarrow 0$, we get

$$\begin{cases} S_{\bar{x}\bar{x}} + 1 = S_{\bar{x}} \\ S(0) = 0 \end{cases}$$

and thus

$$S(\bar{x}) = c_1 e^{\bar{x}} - c_1 + \bar{x}, \quad c_1 \in \mathbb{R}.$$

Therefore, in outer variables we have that

$$\hat{T}(\hat{x}) = \varepsilon S(\bar{x}) = \varepsilon c_1 e^{\bar{x}} - \varepsilon c_1 + \varepsilon \bar{x} = \varepsilon c_1 e^{\frac{\hat{x}}{\varepsilon}} - \varepsilon c_1 + \hat{x}$$

Since $\hat{x} = \mathcal{O}(\varepsilon)$, we have that the leading order term is \hat{x} . Hence, the inner expansion is

$$\hat{T}(\hat{x}) = \hat{x}$$

that clearly satisfies the inner boundary condition $\hat{T}(0) = 0$.

Matching Note that the constant c_0 in the outer expansion has not been determined yet. We solve this by matching the outer and inner expansions at $\hat{x} = 0$, thus we obtain

$$c_0 = -1.$$

Finally, we have that

$$\begin{cases} \hat{T}(\hat{x}) = -e^{-\hat{x}} + 1, & \hat{x} \gg \mathcal{O}(\varepsilon) \\ \hat{T}(\hat{x}) = \hat{x}, & \hat{x} = \mathcal{O}(\varepsilon) \end{cases}$$

Equivalently, expressed in terms of the initial variables T and x , we get

$$\begin{cases} T(x) = (T^c - T_{ini})(1 - e^{-\frac{2hD}{Rku}x}) + T_{ini}, & x \gg \mathcal{O}(\frac{D}{u}) \\ T(x) = (T^c - T_{ini})\frac{2hD}{Rku}x + T_{ini}, & x = \mathcal{O}(\frac{D}{u}) \end{cases}$$

5.3 Solving an instance of our model

This subsection concentrates on solving in instance of our model with our convection-diffusion equation.

First of all we will consider the boundary and initial conditions:

$$\begin{cases} \tilde{T}(0, t) = 293 \\ \tilde{T}(x, 0) = 293 \\ \lim_{x \rightarrow \infty} \tilde{T}_x = 0 \end{cases} \quad (41)$$

Thus, we are supposing that water enters the pipe with a temperature of 293 kelvins, and that far enough along the pipe, temperature does not change. We will also suppose that initial temperature of the water throughout the whole pipe is also 293 kelvins.

As this problem can not be solved analytically with the basic PDE solving methods, we will focus on the numerical solution. First of all, let us define the IVP

$$\begin{cases} \tilde{T}_t + u\tilde{T}_x = D\tilde{T}_{xx} + \frac{2D}{Rk}h(T^c - \tilde{T}) \\ \tilde{T}(0, t) = 293 \\ \tilde{T}(x, 0) = 293 \\ \lim_{x \rightarrow \infty} \tilde{T}_x = 0 \end{cases} \quad (42)$$

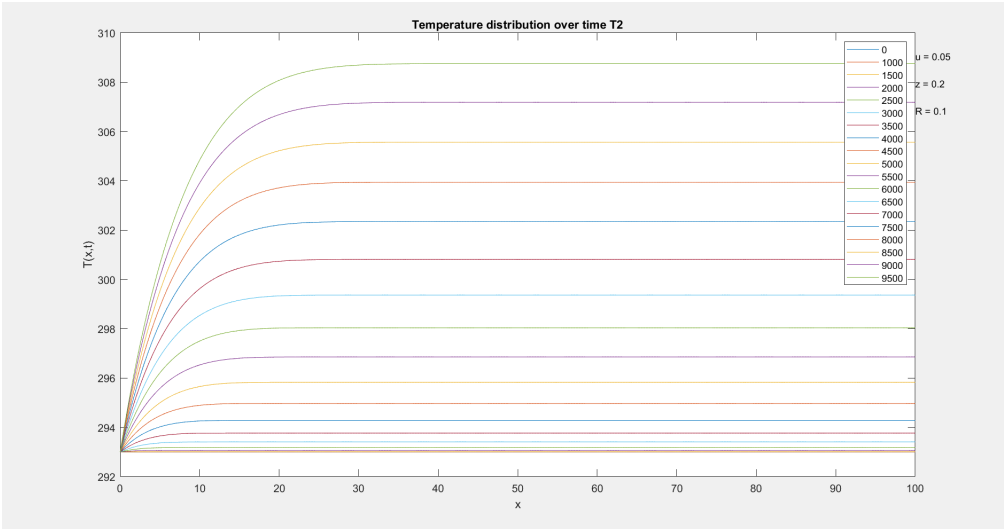
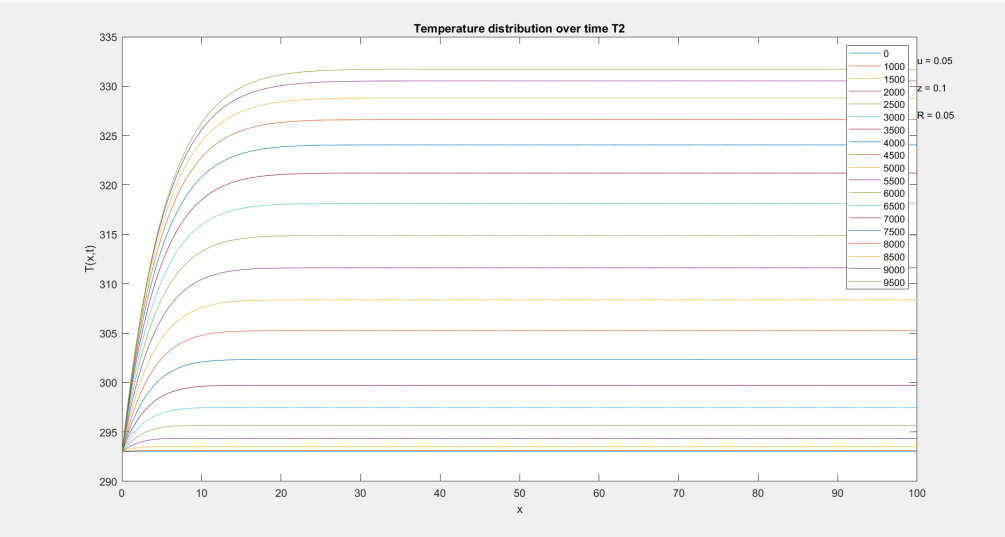
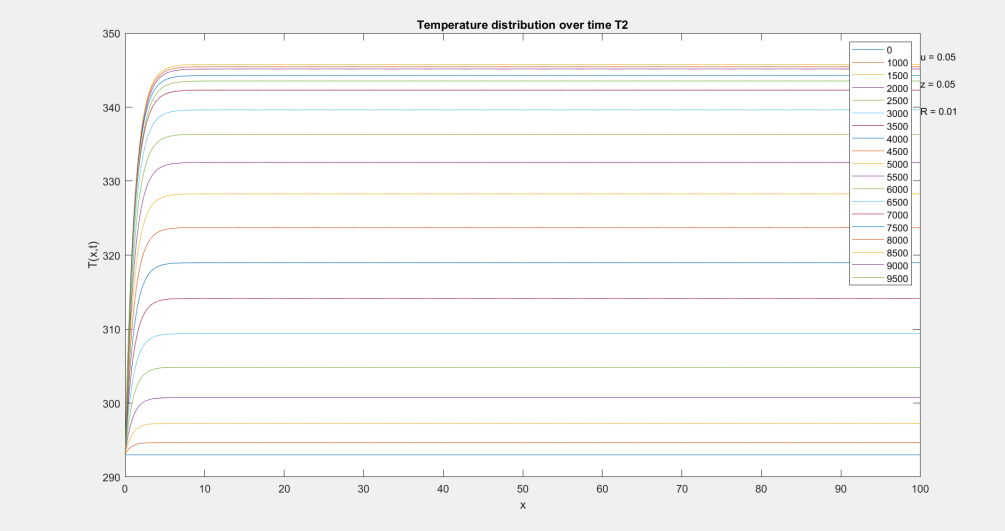
where ($D = \frac{k}{\rho c}$). We will take the solution of the equation that models the heat propagating through the concrete, with the quadratic function for the solar radiation term.

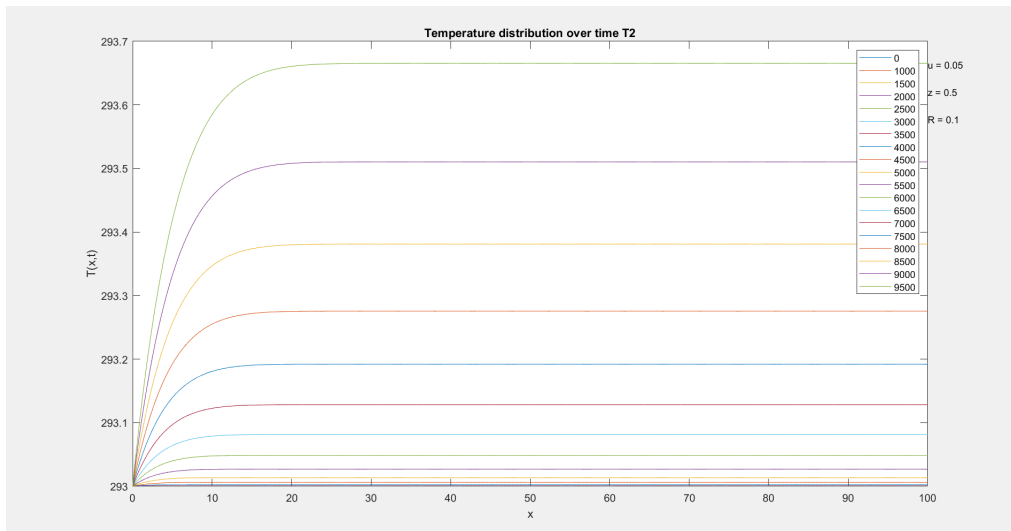
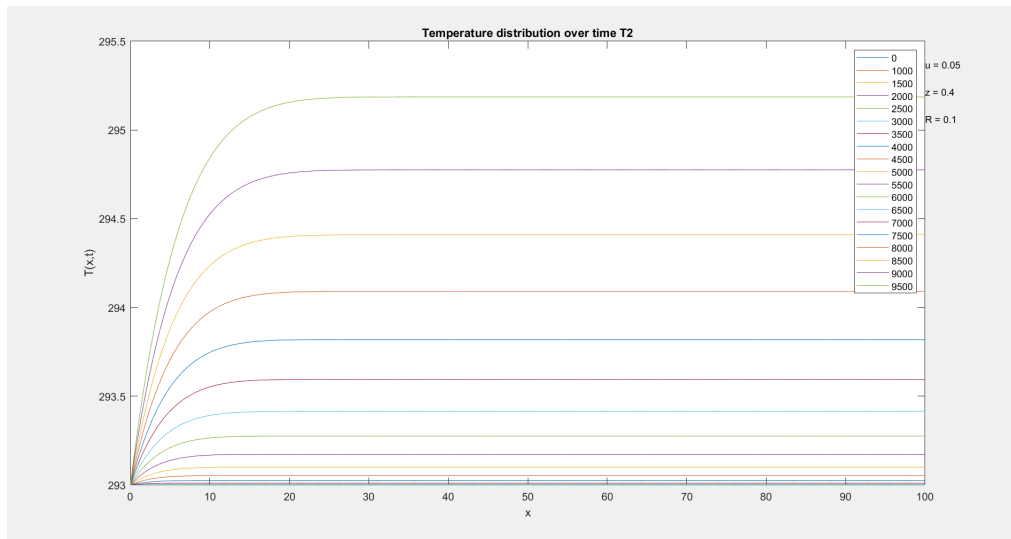
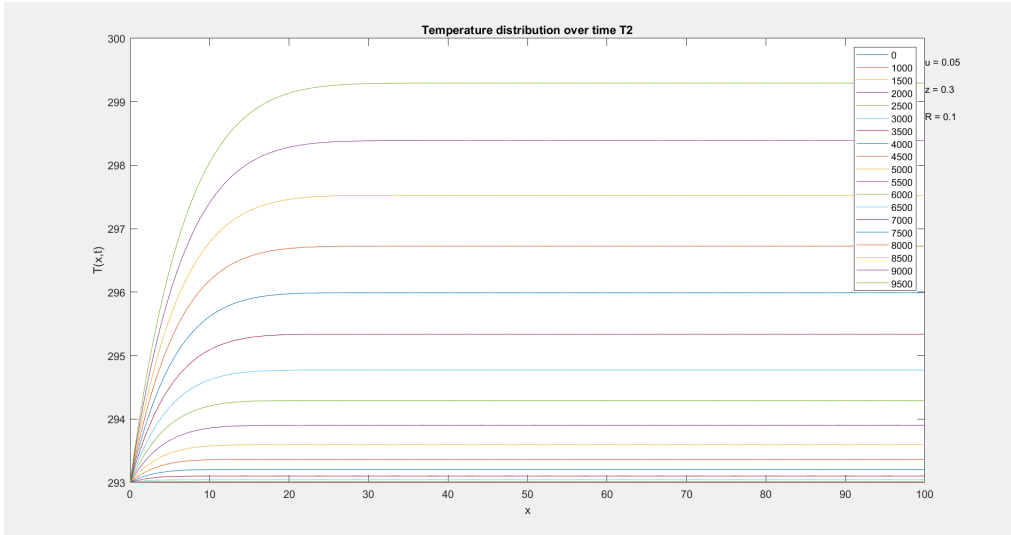
To resolve the convection-diffusion equation, we employed the finite differences method. This approach yielded solutions given water velocity “u”, pipe radius “R”, and depth of the pipe “z”, transforming the partial differential equation (PDE) into a system of ordinary differential equations (ODEs). While the Euler method was initially considered to solve the (ODEs) system, divergence issues usually appeared for certain parameter values. To mitigate this, we adopted the backward Euler method, which, despite its higher computational demands, effectively prevented solution divergence. It is important to take into account that the radius R must always be smaller than z , as otherwise the pipe would be protruding from the ground.

The solution is observed over a 16-hour period, representing daylight hours. Furthermore, we chose a large pipe length, denoted by L , to provide a reliable representation of the null Neumann condition that we have. This methodology underscores the impact of parameters like “u”, “R”, and “z” on the temperature distribution within the pipe.

Below there are some graphics for different scenarios. It is important to note that for some solutions L changes, because for small L in some cases problem could not be solved. If “u” is quite big (greater than 5, L must be bigger than 7000).

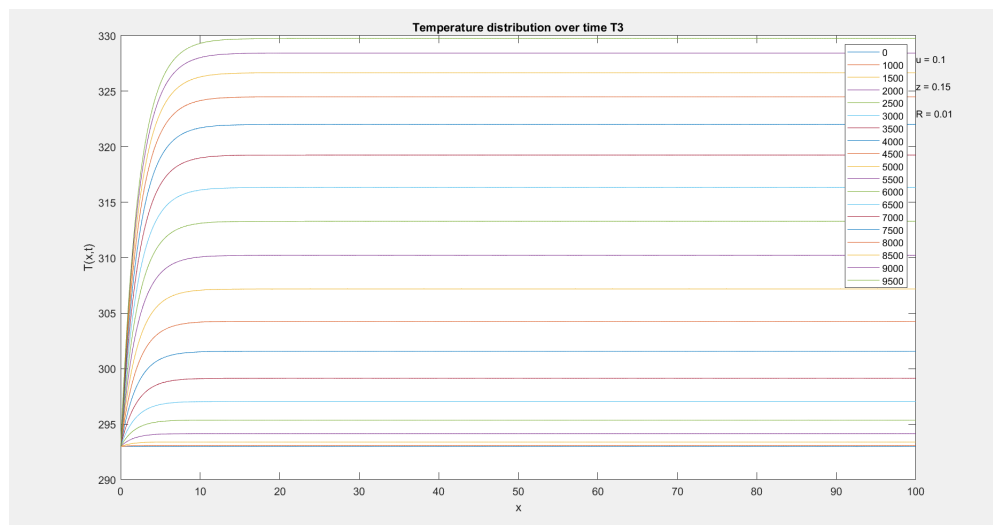
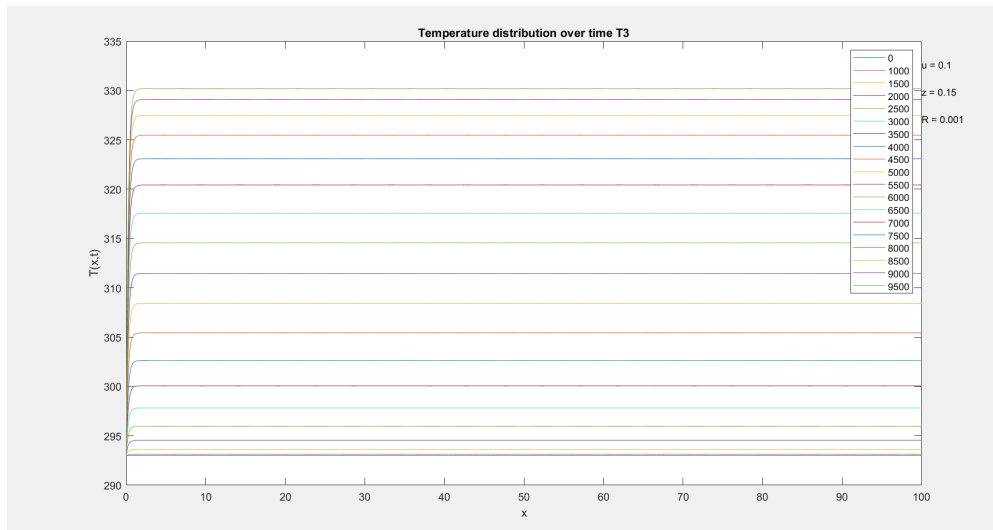
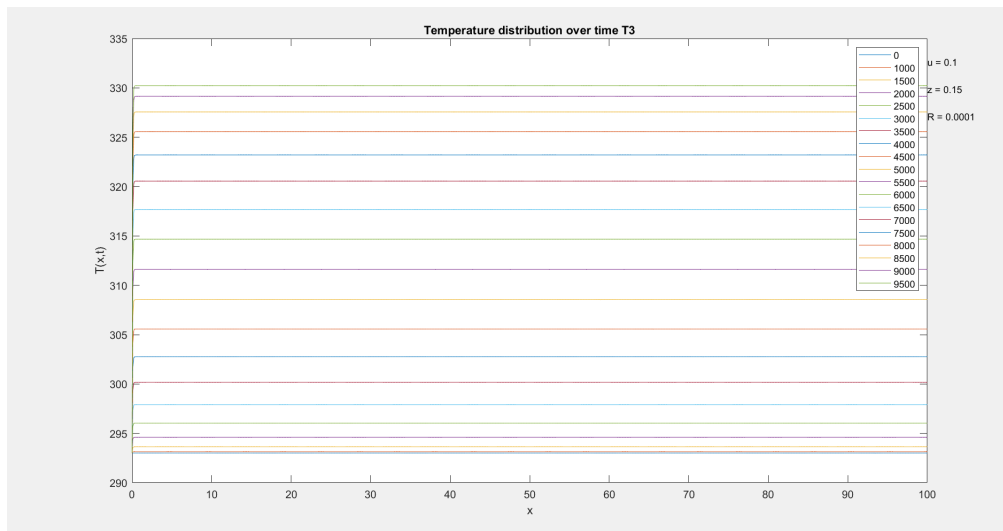
On the one hand, We can see the evolution of how temperature increasing fluctuates a lot between “z=0” and “z=0.5”, also proving that for z exceeding 0.5, we can assume water does not increase.

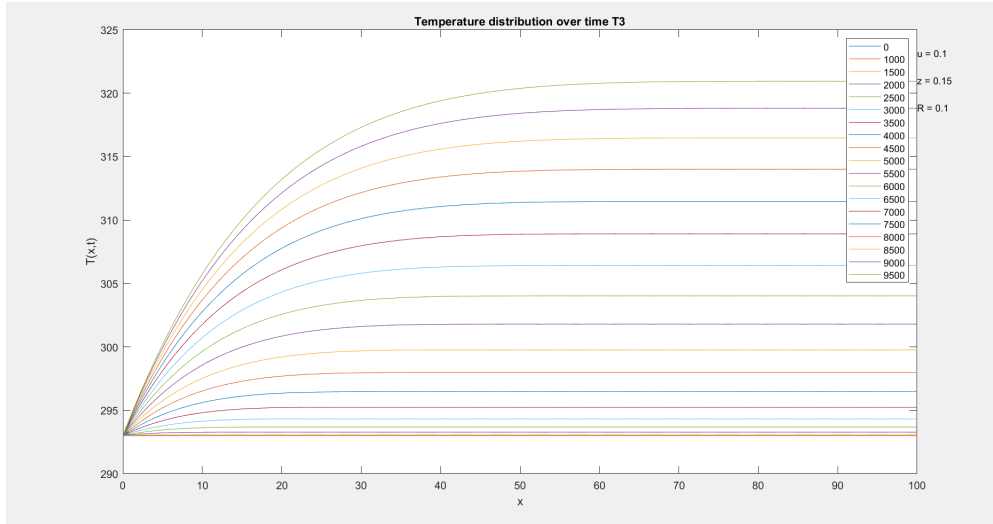




On the other hand, we also study how solution changes as “u” increases, keeping “R”

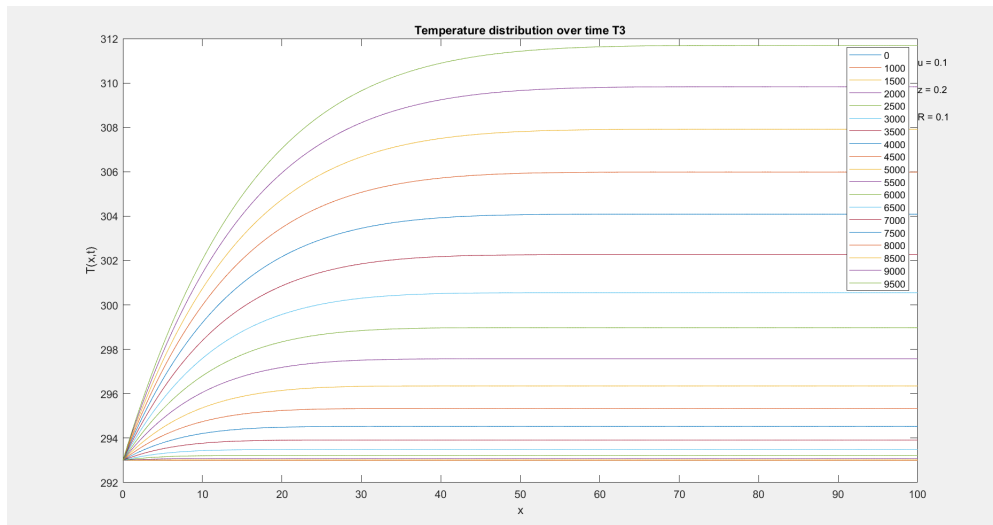
and “z” constant, as in the same way we decrease “R” keeping constant “u” and “z”.

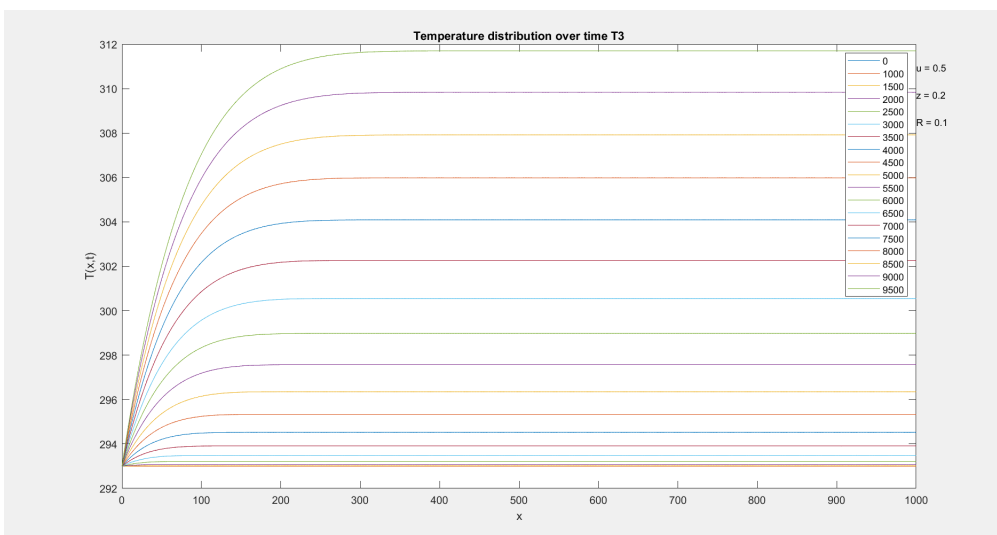
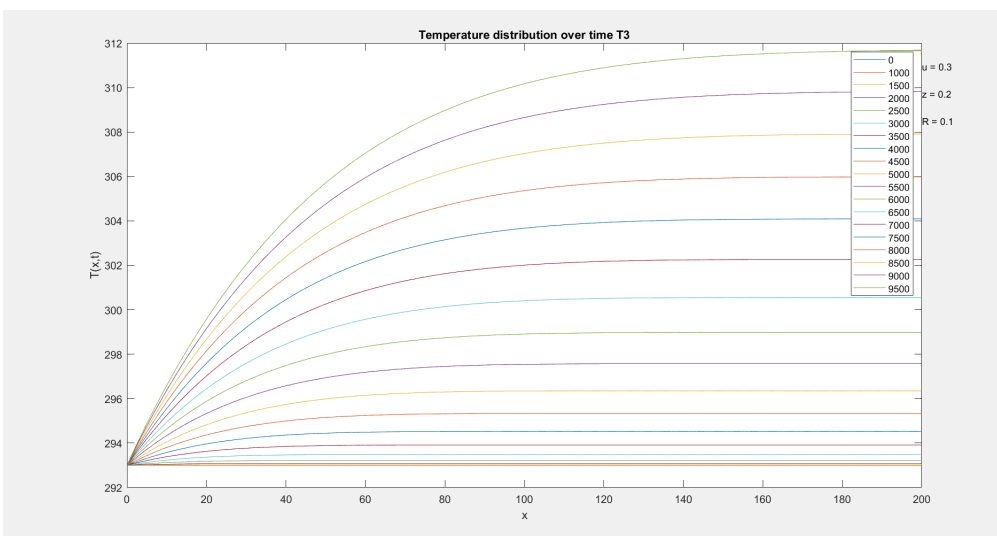
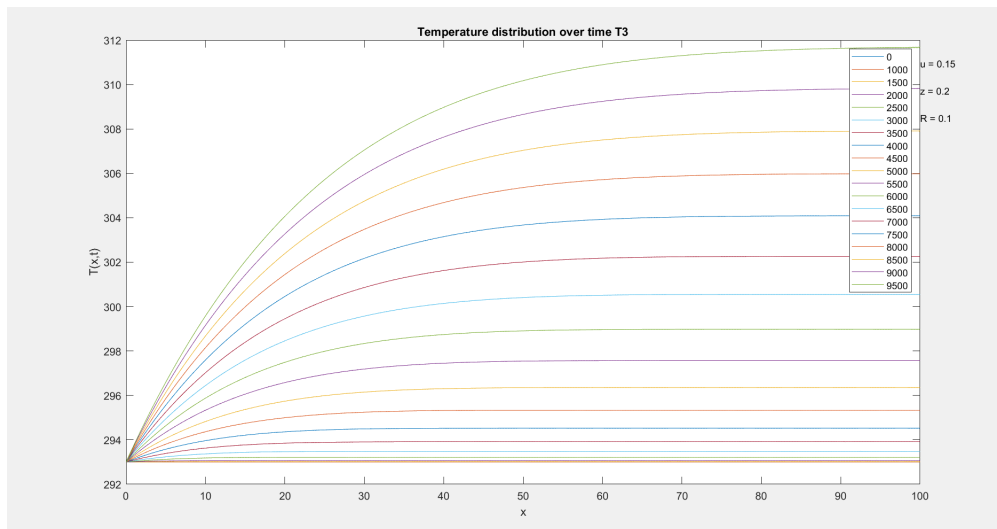


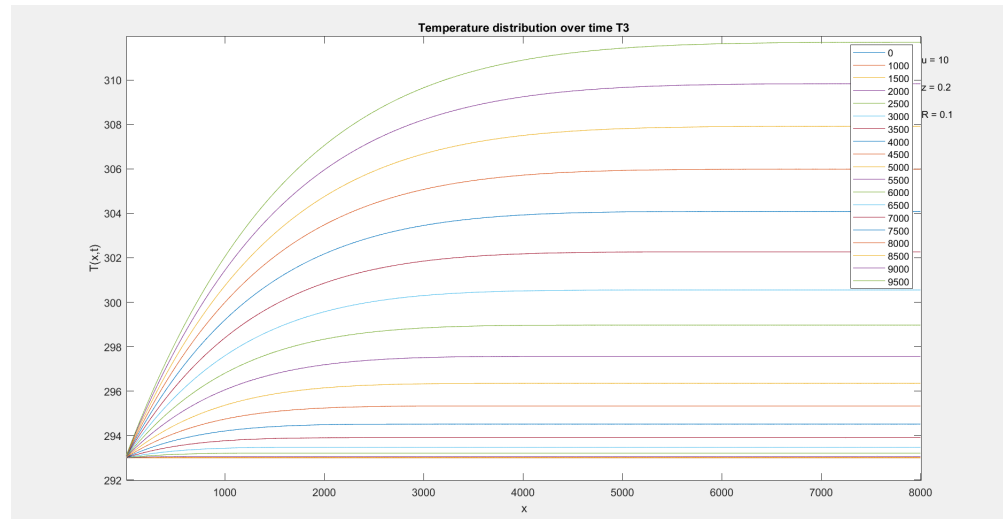
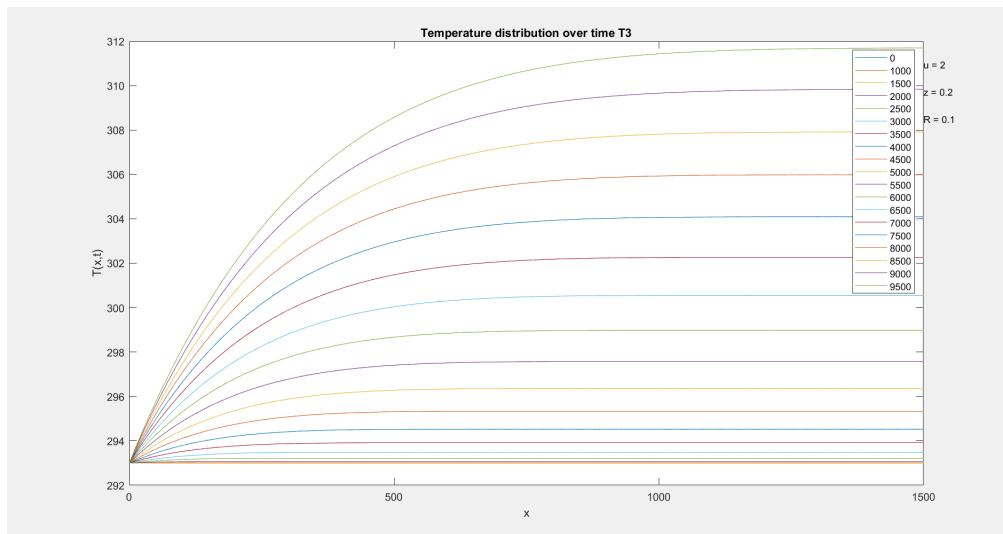
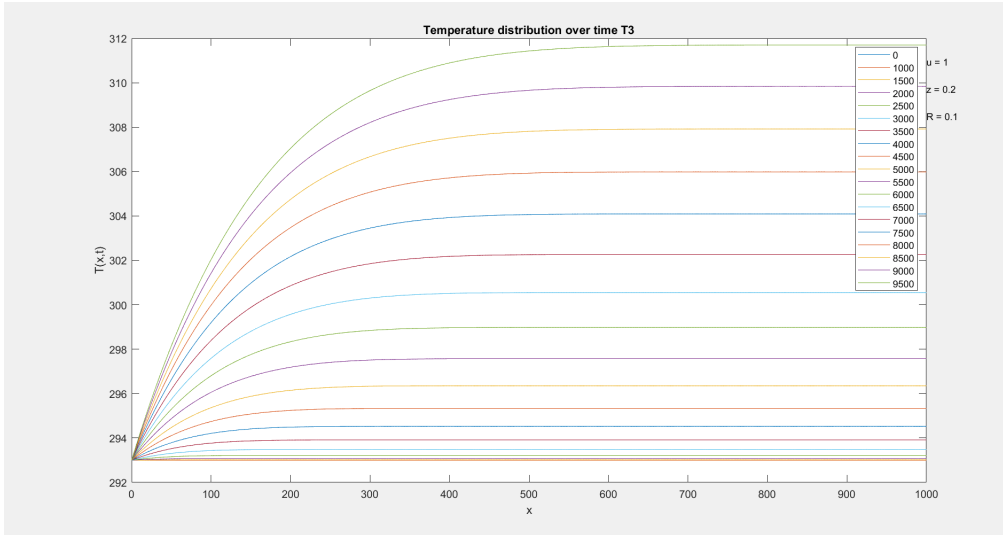


Until here, we have increased the radius from “ $R = 0.0001$ ” to “ $R = 0.1$ ”. We can extract the conclusion that the water temperature which is reached for each time does not change, but it is heated slower.

In the following cases we will increase “ u ” keeping radius and depth constant.







(We must take into account that L parameter changes in the majority of the problems)

We can observe that values of “u” and “R” are the primary factors causing the temperature stabilization curve to require more meters of piping. While when we only increases “u” we need to increase L as well. If we do not increase L, time curve can not be stabilized and consequently problem does not accept a solution.

6 Alternate approaches during our research

This section showcases alternative approaches explored during our research, which were not included in the initial part of the report. These models, while informative, were based on certain assumptions that proved to be less accurate or included elements that did not significantly contribute to our final results. Nevertheless, we believe it's beneficial to present these efforts in their entirety to provide a comprehensive view of the entire research process

6.1 Solving the non-homogeneous heat equation for a concrete structure

In this subsection, we explore the modeling of solar heat transfer into concrete, asphalt, or brick road structures. This process involves solving the non-homogeneous heat equation, which is formulated based on the specific physical properties of these materials. The equation is expressed as:

$$\rho_c c_c T_t = K_c T_{xx} - \frac{2Q_c}{R_c} \quad (43)$$

Here, ρ_c , c_c , K_c , Q_c , and R_c denote the material-specific constants. The goal is to understand how this heat transfer in the road material influences the temperature within a water pipe located beneath the road surface, as in the previous chapter. We address this by setting up and solving the appropriate initial value problem (IVP), ensuring the solution is relevant to the physical scenario at hand.

In the process of non-dimensionalizing the variables in our model, we simplify the non-homogeneous heat equation to

$$\hat{T}_t = \hat{T}_{xx} + C, \quad C := -\frac{2Q_c}{R_c}. \quad (44)$$

This equation reflects the reformulated variables, with C being a composite constant derived solely from Q_c and R_c . To set up the initial value problem (IVP) for this equa-

tion, we define a new function $Q(x, t) = \hat{T}(x, t) - 1$ for ease of computation. The IVP, considering the boundary conditions, is given by:

$$\begin{cases} Q_t = Q_{xx} + C \\ Q(0, t) = 0 \\ Q_x(L, t) = 0 \\ Q(x, 0) = -1 \end{cases} \quad (45)$$

Here, L represents the length of the pipe, and we are within a finite domain. We aim to find a solution akin to that of the homogeneous problem, structured as a series in terms of sine functions due to their orthonormal properties in this context.

The constant C in our model is expanded using Fourier series by the equation

$$C = \sum_{k=0}^{\infty} c_k \sin(\sqrt{\lambda_k} x), \quad c_k = \frac{4C}{\pi(2k+1)} \quad (46)$$

The Fourier coefficients c_k are computed in the usual manner. Integrating this with our initial problem, we arrive at a new equation:

$$\sum_{k=0}^{\infty} B'_k(t) \sin(\sqrt{\lambda_k} x) = \sum_{k=0}^{\infty} (c_k - B_k(t) \lambda_k) \sin(\sqrt{\lambda_k} x), \quad Q(x, 0) = -1 \quad (47)$$

This leads to a simplified ordinary differential equation (ODE):

$$\begin{cases} B'_k = c_k - \lambda_k B_k \\ B_k(0) = -\frac{4}{\pi(2k+1)} \end{cases} \quad (48)$$

Solving this ODE and applying the initial value, we obtain:

$$B_k(t) = e^{-\lambda_k t} \left(\frac{c_k(e^{\lambda_k t} - 1)}{\lambda_k} - \frac{4}{\pi(2k+1)} \right) \quad (49)$$

Thus, we have successfully derived our solution, which is expressed as:

$$T(x, t) = 1 + \sum_{k=0}^{\infty} B_k \left(\frac{\rho_c c_c L^2 t}{K_c} \right) \sin \left(\sqrt{\lambda_k} L(x + ut) \right), \quad B_k(t) = e^{-\lambda_k t} \left(\frac{c_k(e^{\lambda_k t} - 1)}{\lambda_k} - \frac{4}{\pi(2k+1)} \right)$$

$$c_k = -\frac{8Q_c}{\pi R_c(2k+1)}, \quad \lambda_k = \left(\frac{(2k+1)\pi}{2L} \right)^2 \quad (50)$$

6.2 Solving the non-homogeneous heat equation in a semi-infinite domain

When extending the non-homogeneous heat equation to an unbounded spatial domain for x , we encounter a scenario similar to the one discussed previously, but with a modification in the second boundary condition. This alteration is necessary to accommodate the infinite extent of x , thereby adjusting our approach to solve the problem while maintaining the core principles of the heat transfer model. The new system is given by:

$$\begin{cases} \hat{T}_t = \hat{T}_{xx} + C \\ \hat{T}(0, t) = 1 \\ \lim_{x \rightarrow \infty} \hat{T}_x(x, t) = 0 \\ \hat{T}(x, 0) = 0 \end{cases} \quad (51)$$

Similar to our approach with the homogeneous problem, we will utilize the Laplace transform to convert the non-homogeneous heat equation into an ordinary differential equation (ODE) that can be more readily solved. This transformation takes into account the initial conditions that arise from the boundary conditions of the original partial differential equation (PDE). Thus, we get:

$$\begin{cases} \frac{\partial^2}{\partial x^2} \tilde{T}(x, s) = s\tilde{T}(x, s) + \frac{C}{s} \\ \tilde{T}(0, s) = 1/s \\ \lim_{x \rightarrow \infty} \tilde{T}_x(x, s) = 0 \end{cases} \quad (52)$$

Initially, solving the homogeneous part of the equation yields:

$$\tilde{T}h(x, s) = Ae^{-x\sqrt{s}} \quad (53)$$

In search of a particular solution, we find:

$$\tilde{T}p(x, s) = -\frac{C}{s^2} \quad (54)$$

When the initial conditions are applied, the general solution of the ODE is obtained as:

$$\tilde{T}_p(x, s) = \frac{1}{s}(1 - \frac{C}{s})e^{-x\sqrt{s}} + \frac{C}{s^2} \quad (55)$$

To finalize, performing the inverse Laplace transform gives us the solution to our initial PDE problem:

$$\hat{T}(x, t) = \frac{C\sqrt{t}xe^{-\frac{x^2}{4t}}}{\sqrt{\pi}} + C\text{erf}\left(\frac{x}{2\sqrt{t}}\right) + \frac{Cx^2\text{erf}\left(\frac{x}{2\sqrt{t}}\right)}{2} - \frac{Cx^2}{2} - \text{erf}\left(\frac{x}{2\sqrt{t}}\right) + 1 \quad (56)$$

If we draw the solution we can observe how it satisfies the equation and its boundary conditions:

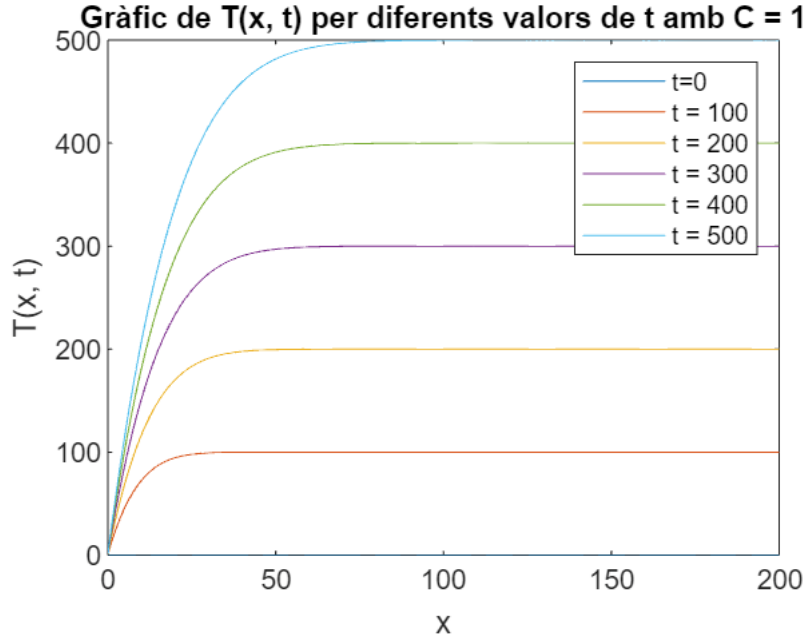


Figure 1: evolution of $\hat{T}(x, t)$ for $t \in [0, 500]$

While our example does not definitively prove that the solution meets all boundary conditions, a closer examination with a "zoomed in" view on smaller values of t clearly demonstrates that $\hat{T}(x, t)$ is indeed the solution to our problem. This approach highlights how specific visualizations can reinforce the validity of our mathematical solutions in practical scenarios.

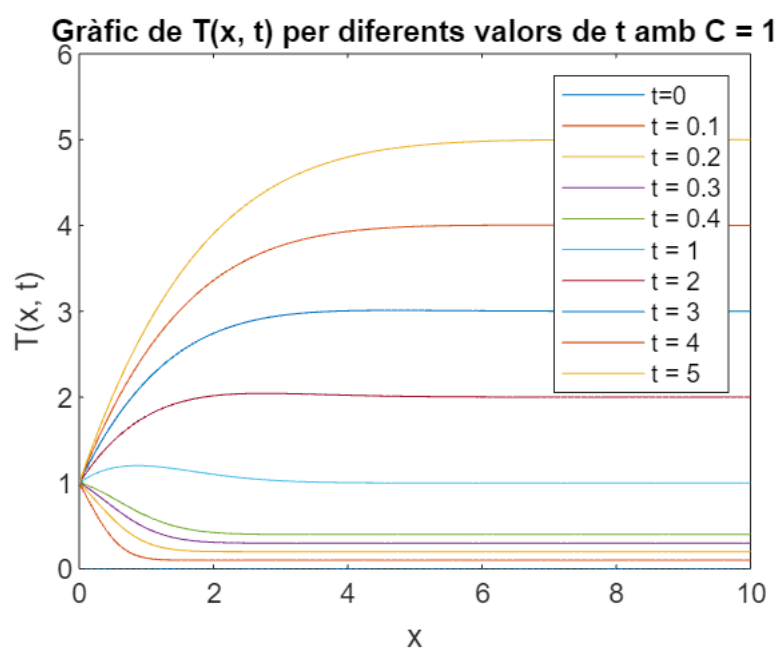


Figure 2: evolution of $\hat{T}(x, t)$ for $t \in [0, 5]$

7 Conclusions

In this report, we studied the use of water pipes under city roads to extract energy from the surfaces, to decrease the urban heat island effect, effectively reducing global warming. Firstly, we modelled the manner in which a fluid in movement heats up in a pipe. Then, we modelled the effect of solar radiation on a city road, incorporating different solar radiation terms to obtain the most realistic model. Consequently, we combined these two models to achieve our complete model, modelling the heat distribution in water pipes under a concrete road, due to solar radiation. This model is given by the following PDE

$$\boxed{\rho c(\tilde{T}_t + u\tilde{T}_x) = k\tilde{T}_{xx} - \frac{2}{R}h\tilde{T} + \frac{2}{R}hT^c} \quad (57)$$

where $T^c(z, t)$ is the temperature of the road material at the specified depth "z", where the pipe will be located.

We have performed the calculations based on the assumption that our surface is made of concrete, due to its excellent properties in absorbing and propagating heat. Additionally, it is a material frequently used in real life, adding more realism to the model. Although asphalt is also commonly used in cities to construct roads, we have ruled it out as a material to use because it absorbs a significant amount of heat. While it would heat the water more, it would contribute to generating more global warming as well. We can not forget that one of the goals of the project was reducing it too, and choosing concrete over asphalt significantly contributes to achieving this goal.

Using, amongst others, this model, although we would have wanted to set optimal values for the depth "z", radius of the pipe "R" and velocity of the running water "u", we only could get some deductions for each parameter as it is explained in Section 5.3. Thanks to numerically solving (57) with different values for "z", "R" and "u" we reached the following conclusions:

- For a given radius and velocity, the closer "z" is to zero, the faster the water's temperature rises and the higher it stabilizes, indicating more efficient energy extraction from the concrete. However, we cannot place the pipe arbitrarily close to the road surface. The minimum depth "z" must be greater than or equal to the radius "R"

to ensure proper pipe placement. Furthermore, placing the pipe directly under the road is impractical due to vibration-induced breakage. Future research should focus on determining the minimum depth at which the pipe can be embedded without compromising its integrity.

- Concerning the radius, we deduce that an increase in it, by increasing the water flow rate, causes the interior of the pipeline to augment its temperature more slowly. Therefore, we will need more meters of pipeline for it to stabilize. We can reduce the radius to prevent this, but, analogously, we will heat less water, and thus the extracted energy will be lower.
- Regarding the velocity, we obtain a similar conclusion; at higher water speeds, it will have less time to heat up, and therefore, more length will be needed for it to stabilize its temperature. We can also reduce its speed, but this will also result in less water circulation, and hence, the amount of generated energy will be lower.

In summary, we could seek the minimum depth to prevent the pipeline from breaking, assuming that vehicles can circulate on the surface. Finally, given the energy we want to generate, we would find the smallest possible radius and velocity that represent the minimum investment in materials.

Regarding the mathematical approaches during our research, we deduced that the Laplace transformation was the most effective way to solve our differential equations analytically, as it also allows you to solve equations on semi-infinite domains. Moreover, we have seen during our research that the modelling was a strong trade-off between the complexity of the model (more realistic), and the tractability of it. We have concluded that in certain cases, as in our solar radiation term, you may have to sacrifice a bit of realism, to retain a manageable model.

8 References

Apart from the guidance and advice received from Tim and the usage of some mathematical programming tools such as *Matlab* or *Wolfram Alpha* to mainly solve and plot the solution to various PDEs (analytically and numerically), we used these references to complement our report:

- [1] Myers, T. G., N. D. Fowkes, and Y. Ballim. “*Modeling the cooling of concrete by piped water.*” *Journal of engineering mechanics* 135.12 (2009): 1375-1383.
- [2] Aguiar, Maria, et al. “*A mathematical model for the energy stored in green roofs.*” *Applied Mathematical Modelling* 115 (2023): 513-540.
- [3] Myers, T. G., and J. P. F. Charpin. “*Modelling the temperature, maturity and moisture content in a drying concrete block.*” *Mathematics-in-Industry Case Studies* 1 (2008).
- [4] Charpin, J. P. D., et al. “*Modeling surface heat exchanges from a concrete block into the environment.*” *Mathematics in Industry* (2004).

9 Appendix

We show here the *Matlab* code we used to solve numerically the PDE from section 3.3, which uses the *pdepe* package:

```
function pde_solver
    L = 1;           % Length of the spatial domain
    x = linspace(0, L, 100); % Spatial grid
    t = linspace(0, 10, 100); % Time grid

    sol = pdepe(0, @pde_eqn, @pde_initial, @pde_boundary, x, t);

    % Extract the solution
    T = sol(:, :, 1);

    % Plot all the solutions together in a single graph
    figure;
    hold on;
    for i = 1:length(t)
        plot(x, T(i, :), 'LineWidth', 1.5);
    end
    hold off;

    title('Solution of PDE at Different Times');
    xlabel('x');
    ylabel('T');
    grid on;
end

function [c, f, s] = pde_eqn(x, t, u, dudx)
    c = 1; % Coefficient in front of the second spatial derivative
    f = -u+dudx; % Coefficient in front of the first spatial derivative
    s = 1; % Source term
end

function u0 = pde_initial(x)
    u0 = 0; % Initial condition
```


end

```
function [pl, ql, pr, qr] = pde_boundary(xl, ul, xr, ur, t)
    pl = ul; % Left boundary condition (Dirichlet at x=0)
    ql = 0;
    pr = ur; % Right boundary condition (Neumann at x=1)
    qr = 1; % Specify the Neumann condition using ql and qr
end
```

We also include here the full analytical solution we got with online calculators for $\hat{T}(z, t)$ (later $T^c(z, t)$) of section 4.2:

$$\begin{aligned} \hat{T}(z, t) = & \frac{ad^4 z^5 \operatorname{erf}\left(\frac{dz}{2k\sqrt{t}}\right)}{60k^5} - \frac{ad^4 z^5}{60k^5} + \frac{ad^3 \sqrt{t} z^4 e^{-\frac{d^2 z^2}{4k^2 t}}}{30\sqrt{\pi}k^4} + \frac{ad^2 t z^3 \operatorname{erf}\left(\frac{dz}{2k\sqrt{t}}\right)}{3k^3} - \frac{ad^2 t z^3}{3k^3} + \frac{3adt^{\frac{3}{2}} z^2 e^{-\frac{d^2 z^2}{4k^2 t}}}{5\sqrt{\pi}k^2} + \\ & + \frac{at^2 z \operatorname{erf}\left(\frac{dz}{2k\sqrt{t}}\right)}{k} - \frac{at^2 z}{k} + \frac{16at^{\frac{5}{2}} e^{-\frac{d^2 z^2}{4k^2 t}}}{15\sqrt{\pi}d} + \frac{bd^2 z^3 \operatorname{erf}\left(\frac{dz}{2k\sqrt{t}}\right)}{6k^3} - \frac{bd^2 z^3}{6k^3} + \frac{bd\sqrt{t} z^2 e^{-\frac{d^2 z^2}{4k^2 t}}}{3\sqrt{\pi}k^2} + \frac{btz \operatorname{erf}\left(\frac{dz}{2k\sqrt{t}}\right)}{k} - \\ & - \frac{btz}{k} + \frac{4bt^{\frac{3}{2}} e^{-\frac{d^2 z^2}{4k^2 t}}}{3\sqrt{\pi}d} + \frac{rz \operatorname{erf}\left(\frac{dz}{2k\sqrt{t}}\right)}{k} - \frac{rz}{k} + \frac{2r\sqrt{t} e^{-\frac{d^2 z^2}{4k^2 t}}}{\sqrt{\pi}d} + T_\infty \end{aligned}$$

Where $\operatorname{erf}(x) = \frac{2}{\sqrt{\pi}} \int_0^x e^{-t^2} dt$, $d := \sqrt{\rho ck}$ and $a, b, r \in \mathbb{R}$ are the coefficients of the considered polynomial $Q_{sun}(t) = at^2 + bt + r$.

